Front. Earth Sci. 2020, 14(4): 738–757
https://doi.org/10.1007/s11707-019-0810-8

RESEARCH ARTICLE

Chemical geothermometry: application to mud volcanic waters of the Caucasus region

Olga E. KIKVADZE (✉)[1,2], Vasilii Yu. LAVRUSHIN[1,2], Boris G. POLYAK[1]

1 Geological Institute, Russian Academy of Sciences, Moscow 119017, Russia
2 V.S.Sobolev Institute of Geology and Mineralogy, Siberian Branch of the RAS, Novosibirsk 630090, Russia

Abstract The generation temperatures of gas-water fluids released from mud volcanoes in different provinces of the Caucasian region have been constrained using Mg/Li ($T_{Mg/Li}$) chemical geothermometry. Mud volcanic fluids in the Taman Peninsula (Kerch-Taman mud volcanic province) were generated at temperatures ($T_{Mg/Li}$) from 41°C to 137°C. The depths of the respective mud reservoirs estimated from $T_{Mg/Li}$ values and local geothermal gradient are in a range of 1.0 to 3.4 km which spans the Maykop Formation of marine shale. For the South Caspian province, the $T_{Mg/Li}$ values of waters vary from 18°C to 137°C and the respective root depths $H_{Mg/Li}$ of mud volcanoes range from ~ 0.85 to 6.5 km. The obtained $T_{Mg/Li}$ values for the analyzed mud volcanic waters from Caucasian provinces are in positive correlation with HCO_3^- contents and water oxygen isotope compositions ($\delta^{18}O_{H_2O}$ and $\Delta\delta^{18}O_{H_2O}$) and in high negative correlation with Cl^-. The increase of $T_{Mg/Li}$ toward the Greater Caucasus Range, as well as the lateral $T_{Mg/Li}$ patterns in the Taman and South Caspian mud volcanic provinces, support the idea that mud volcanic fluids generate at temperatures increasing progressively toward the Alpine orogenic belt.

Keywords mud volcano, fluid, chemical geothermometry, stable isotopes, Caucasus region

1 Introduction

Mud volcanoes (MVs) are specific landforms created by extrusion and eruption of liquefied mud, saline water and gases (mainly methane and CO_2). They are common to many sedimentary basins in compressional settings, including intermontane basins within young orogenic belts, like the Caucasus, South Caspian Basin, and Mediterranean regions (Jakubov et al., 1971; Dimitrov, 2002; Kopf, 2002; Mazzini et al., 2009; Oppo et al., 2014; Mazzini and Etiope, 2017). More than 1500 onshore and offshore mud volcanoes worldwide cluster in mud volcanic provinces and are normally dormant but discharge mud volcanic fluids (MVF) (Milkov, 2000; Dimitrov, 2002; Kopf et al., 2003; Kholodov, 2013; Mazzini and Etiope, 2017). The sources of the fluids and their generation temperatures, as well as the depths of the feeding mud chambers and roots, remain poorly understood (Kholodov, 2002 and 2013; Kopf, 2002; Kopf et al., 2003; Mazzini et al., 2009; Etiope, 2015; Kokh et al., 2017; Mazzini and Etiope, 2017).

Mud volcanoes are abundant in the Caucasus segment of the Alpine-Himalayan belt, with at least 400 edifices in the Indol-Kuban Trough (Russia) and the Kura intermontane basin that comprises the Middle (East Georgia) and Lower (Azerbaijan) Kura subbasins. The Lower Kura basin, known for offshore mud volcanism, borders the Caspian Sea. The total sediment thickness in the South Caspian basin exceeds 20–25 km, while the MV roots exceed 8–9 km (Jakubov et al., 1980; Rakhmanov, 1987; Guliev et al., 1988; Nadirov et al., 1997; Ali-Zade, 2008; Sobissevitch et al., 2008). Fluid systems at these depths are hardly accessible for drilling and remain most often uninvestigated. The chemistry of MV fluids has implications for the compositions of sediments and their maturation conditions, as well as for the origin depths and generation mechanisms of fluids. The respective reconstructions can bridge the gaps of knowledge on diagenesis and maturation processes.

The depths of mud reservoirs can be inferred from constrained MV fluid generation temperatures and the known local temperature gradients. Waters released from dormant mud volcanoes have permanently low temperatures of 10°C to 30°C. However, the measured *in situ*

Received October 14, 2018; accepted November 25, 2019

E-mail: bolik2000@mail.ru

temperatures of emergent MV waters in salsas and gryphones are not the true subsurface water temperatures: the ascending waters cool down under an adiabatic effect of gas expansion or as a result of seasonal and diurnal air temperature variations.

Although the temperatures of emergent mud volcanic waters provide no idea of their initial values at origin depths, these values can be constrained by chemical geothermometry. Calibrated water geothermometers were developed in the 1960-1980-s and used for temperature estimation in geothermal systems and diagenetically altered sediments (Bödvarsson, 1961; Bödvarsson and Pálmason, 1961; Fournier and Truesdell, 1973; Fournier, 1977; Fouillac and Michard, 1981; Kharaka and Mariner, 1989). Geothermometry stems from empirical relationships between element concentrations or their ratios in waters and temperatures measured directly in drilled aquifers or reservoirs. Analysis of temperatures measured in subsurface fluids revealed that their warming is coupled with increasing salinity (concentrations of total dissolved solids, TDS). Iceland researchers (Bödvarsson, 1961; Bödvarsson and Pálmason, 1961) proposed the terms base temperature for water temperature at the respective TDS formation level and base depth for the position of the respective isotherm.

Different chemical geothermometers have been proposed to estimate temperatures in both geothermal systems and more or less diagenetically altered rock reservoirs. The SiO_2, Mg/Li, Na/Li, and Na/K geothermometers are most important for reconstructing sediment maturation temperatures, as well as the temperatures of oil and gas reservoirs at the time of fluid generation (Bödvarsson, 1961; Bödvarsson and Pálmason, 1961; Fournier and Truesdell, 1973; Fournier, 1977; Fouillac and Michard, 1981; Kharaka and Mariner, 1989; D'Amore and Arnórsson, 2000). Soon after coming into use, the geothermometers were found out to frequently yield appreciably different reservoir temperatures owing to the lack of equilibrium between the solution and the dissolved/precipitated minerals, or as a result of reactions, mixing or degassing during fluid up-flow. The Na/Li and Mg/Li thermometers yield more reliable estimates than the SiO_2, K/Na, and K/Na/Ca ones because they are less sensitive to host lithology and better suitable for basinal waters (Kharaka and Mariner, 1989; Lavrushin et al., 2003). Qualitative interpretations and constraints on fluid-forming processes and source depths can be obtained using isotopic tools, besides other geochemical fingerprints (D'Amore and Arnórsson, 2000). Water isotopic patterns have implications for the depths of diagenetic alteration in the case of smectite–illite transformation accompanied by release of abundant freshened water into the pore space (Kopf, 2002; Lavrushin et al., 2003; Chelnokov et al., 2018; Sokol et al., 2019).

The geochemical-based approaches to MV fluid generation conditions are especially valuable for the areas not covered yet by petroleum exploration drilling. On the other hand, most of the available studies are limited to restricted MV areas, single edifices, and even single discharges. In this respect, the regional-scale patterns which would reveal general trends with a perspective on mud volcanism over vast territories remain unknown. This paper provides the first comparative analysis of geochemistry and reconstruction of MV water temperature patterns in different parts of the Caucasus region extending over a 1500 km long zone from the Kerch Peninsula in the west to the Caspian Sea in the east. The reconstructions of fluid generation temperatures and respective depths are based on a vast collection of monitoring data from 2009 through 2013. The results were partly published earlier (Kikvadze et al., 2014; Lavrushin et al., 2015), but the greatest portion of data has never been reported before.

2 Geological setting

The present tectonic framework of the Caucasian region results from Late Cenozoic folding and thrusting associated with the continental collision of Eurasia with Africa and Arabia (Khain, 1982; Zonenshain and Le Pichon, 1986; Gamkrelidze and Giorgobiani, 1989; Philip et al., 1989; Leonov, 2007; Mosar et al., 2010; Kadirov et al., 2015). The N–S cross section of the region comprises several major units (Fig. 1): the Indol-Kuban and Terek-Caspian foredeeps, the Great Caucasus Range, and the Kura and Rioni intermontane basins between the Great and Lesser Caucasus systems (Khain, 1982; Philip et al., 1989).

The collisional processes in the southern slope of the Great Caucasus are still active at present. According to GPS data, the area is moving northward at 3–4 mm/yr but the velocity of the Lesser Caucasus and Kura continental blocks is as high as 13 mm/yr (Mosar et al., 2010; Kadirov et al., 2015). The plate motion induces high seismicity, thrusting, and formation of shear zones in the Caucasus southern slope and along the basin borders.

The sedimentary section of the intermontane and foreland basins begins with Early Jurassic strata and encompasses almost all Mesozoic and Cenozoic stratigraphic units. This section includes the Maykop Formation of Oligocene–Early Miocene shale which often constitute almost half of the sediment thickness. For instance, it occupies 5–6 km out of a 13–14 km section in the central Kura basin (Krasnopevtseva et al., 1977; Chelidze, 1983; Iosseliani and Diasamidze, 1983; Adamia, 1985; Radzhabov et al., 1985; Ali-Zade, 2008) or 3–5 km out of 8 to 12 km thick sediments in some parts of the Indol-Kuban Trough (Jakubov et al., 1980; Nadirov et al., 1997; Shnyukov et al., 1986 and 2005; Rakhmanov, 1987). All sedimentary basins of the Caucasus region (except for Rioni) are rich reservoirs and developed pays of oil and gas.

The Caucasus region hosts a great number of active mud

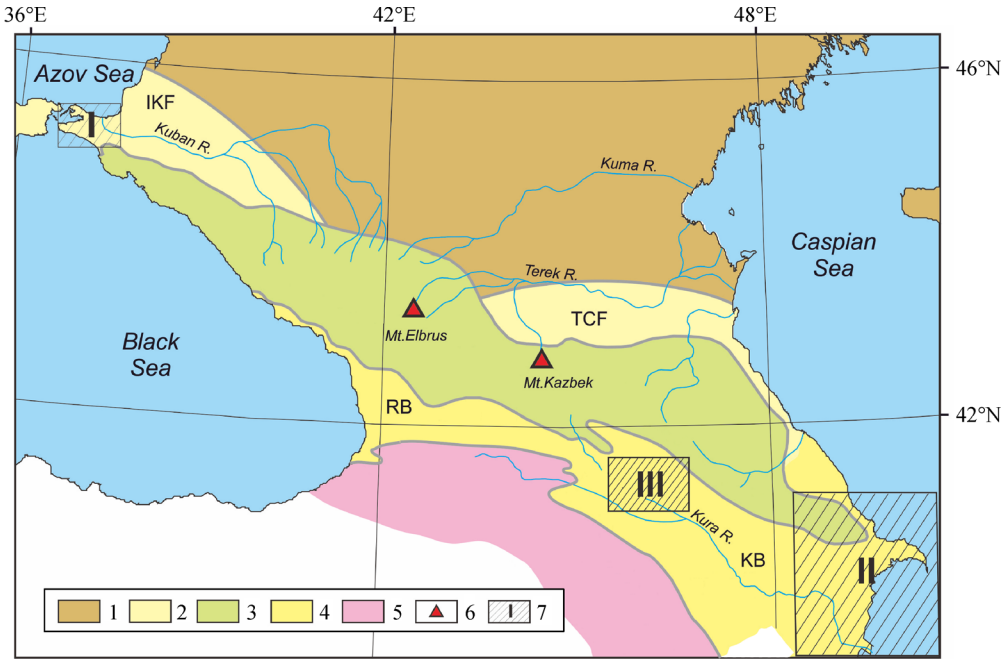

Fig. 1 Tectonic sketch map of Caucasus (simplified after Milanovskii and Koronovskii (1973)). 1 – Scythian Plate; 2 – Indol-Kuban (IKF) and Terek-Caspian (TCF) foredeeps; 3 – Greater Caucasus orogen; 4 – Rioni (RB) and Kura (KB) intermontane basins; 5 – Lesser Caucasus orogen; 6 – centers of recent Ca-alkaline volcanism; 7 – Kerch-Taman (I), South Caspian (II) and Kakhety (III) MV provinces.

volcanoes in mud volcanic provinces that belong to different tectonic units (Fig. 1). The *South Caspian* province is the world largest areas of mud volcanism with more than 180 onshore edifices (Jakubov et al., 1980; Aliyev et al., 2009; Feyzullayev, 2012), and as many offshore volcanoes within the southern Caspian Sea. Most of the edifices belong to the South Caspian sedimentary basin, with the Kura basin as its onshore extension. Mud volcanism in the Kura basin occurs in its Middle and Lower subbasins. The latter accommodates Jurassic and Cretaceous sediments overlain by Cenozoic molasse, 10–12 km thick in total (Guliev et al., 2013), and includes the Fore-Caspian, Apsheron, Shemakha-Gobustan, and Fore-Kura petroleum areas in Azerbaijan (Jakubov et al., 1971). Offshore seismic surveys in the South Caspian Sea allowed tracking feeder channels of mud volcanoes to 8–10 km below the surface, but no onshore data are available (Ali-Zade, 2008; Feyzullayev, 2012).

The Kakhety province has six MVs in its territory and it is located in Eastern Georgia at the transition from the Kura intermontane basin to the Great Caucasus southern slope, where 13–14 km thick consolidated crust is overlain by sediments, including a 4–6 km thick Mesozoic section (Krasnopevtseva et al., 1977; Jakubov et al., 1980; Iosseliani and Diasamidze, 1983; Adamia, 1985; Adamia et al., 2008; Aliyev et al., 2015). The thickest Cenozoic sediments correspond to the Oligocene-Early Miocene Maykop Formation (5–6 km) and the Late Miocene Shirak Formation (2–2.5 km). The large sediment thickness in the Middle Kura basin may be as a result of the presence of multiple thrust complexes (Mosar et al., 2010; Adamia et al., 2011).

Another large MV province, that of *Kerch-Taman*, lies in a zone of thick Pliocene–Quaternary sediments of the Indol-Kuban Trough which borders the Greater Caucasus Range in the north (Fig. 1). Mud volcanism in the region culminated during the Middle Miocene Chokrak and Middle-Late Sarmat deposition events but has decayed lately. Forty out of 80 mud volcanoes in the province are currently active (Shnyukov et al., 1986 and 2005; Kopf et al., 2003; Lavrushin et al., 2003 and 2005; Olenchenko et al., 2015; Sokol et al., 2018 and 2019). The zones of mud volcanism are located in basin borders deformed by folds and thrusts as in the Kura basin.

Thus, there are two main factors favorable for mud volcanism in the Caucasus region: 1) the presence of thick Cenozoic shales of which some are producing oil and gas reservoirs; 2) high activity of Cenozoic and recent geodynamic processes. This combination of factors is typical of many MV provinces worldwide (Kopf, 2002).

3 Materials and Methods

3.1 Sampling

Mud volcanic fluids in the Taman Peninsula and Azerbaijan were monitored during several successive field campaigns of 2009, 2010, 2012, and 2013. Waters were sampled from 14 MVs in the Taman Peninsula in

2009 and from 56 edifices in Azerbaijan (South Caspian province) during the trips of 2010, 2012 and 2013 (Figs. 2 and 3; Tables 1, 2, and S1). Additionally, a flowing abandoned borehole (13-1/10) was sampled at the foot of Neftechala volcano. Our results have been compared with earlier data collected in the September of 1997 from MVs in the Kakhety province (Lavrushin et al., 1996, 2003, and 2005).

The sampled sites were located using a Garmin GPS, in a WGC-84 system (accuracy of 3–5 m). The temperature and pH of every sampled water issue were measured in situ with a manual Hanna Instruments PH ORP Combo Meter & Temperature Gauges (HI98121) to a precision of ±0.1°C and ±0.1 pH. Eh measurements were performed in situ using a Pt electrode, with an EXPERT 001 manual pH-meter, to a precision of ±0.1 mV Eh.

Sampling of water and free emanating gases for laboratory studies were from the most active salsas in the central part of the MV field; at large volcanoes, a central and several side salsas were sampled. The sampling techniques were detailed previously (Kikvadze et al., 2014; Lavrushin et al., 2015).

MV waters were sampled simultaneously into plastic vials and bottles. Water was filtered through a 0.45-μm Nucleopore filter a few hours after sampling, in order to avoid initial salt precipitation and colloid coagulation. Major cations and trace elements were analyzed in 15 water aliquots which were stored separately and then acidified with 0.5 mL of 15N distilled nitric acid; anions were determined in another 50 mL aliquot of unacidified water; other 15 mL water aliquots stored in glass bottles were used for analysis of H and O isotopes. Gas was sampled by pumping using a small water siphon, into 100 cm^3 glass bottles.

3.2 Analytical procedures

Major-element concentrations in water samples were measured at the chemical analytical laboratory of the Geological Institute (GIN, Moscow, Russia) and at the Analytical Center of the Institute of Microelectronics, Technology and High-Purity Materials (IMT, Chernogolovka, Russia), by ICP-AES, ICP-MS, and acid and $AgNO_3$ titration. The analytical details were summarized previously (Lavrushin, 2012; Lavrushin et al., 2015). Trace element compositions were analyzed at IMT (Chernogolovka) on a Thermo Jarrel (USA) and a Thermo Elemental X-7 ICP-MS (USA) analyzers following the procedure from (Karandashev et al., 2016). The accuracy and precision were monitored by measuring the IAPSO salinity standard on a regular basis (Gieskes et al., 1992). The concentrations measured for IAPSO were generally within 5% of seawater values at the salinity on the IAPSO standard bottle. The precision and accuracy were 10 rel%–15 rel% for all analyzed elements.

Water salinity (Table 2) was estimated by summation of main dissolved salts: Na, K, Ca, Mg, Cl, HCO_3 and SO_4.

Oxygen and hydrogen isotope compositions of H_2O were studied at the Laboratory of Isotope Geochemistry and Geochronology of the Geological Institute (Moscow) using Thermoelectron instruments, including a *Delta-V-Advantage* mass spectrometer, and a Finnigan-TC/EA thermochemical element analyzer (for δD in H_2O). All δD and δ^{18}O values are quoted in ‰ relative to the V-SMOW standard. The δ^{18}O and δD estimates are accurate (reproducible) to no worse than ±0.2 ‰ and 3 ‰, respectively. More analytical details were reported earlier (Lavrushin et al., 2015; Pokrovsky et al., 2017). All the results are summarized in Tables 1–2.

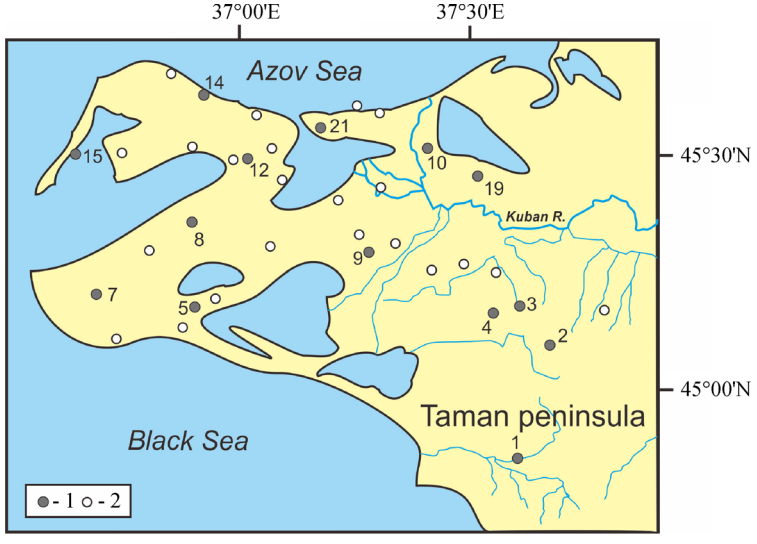

Fig. 2 Location map of mud volcanoes in the Taman peninsula, Kerch-Taman MV province, according to (Shnyukov et al., 1986). 1-2 – sampled 1) and non-sampled 2) mud volcanoes. Sampling sites numbers are same as in Table 1.

Table 1 Locations of sampling sites and oxygen and hydrogen isotope compositions of mud volcanic waters

MV No.	°N lat.	°E long.	Sampling site	Sample number*	VSMOW/ ‰			Data source***
					$\delta^{18}O$	δD	$\Delta\delta^{18}O$**	
Kerch-Taman Province (see Fig. 2)								
1	44.90111	37.59833	Semigor MV	14-1/09	10.3	−25	14.7	1
1	44.90111	37.59833	Semigor MV	14-3/09	10.0	−27	14.6	1
2	45.00561	37.72372	Gladkov MV, seepage 4	2/09BG	5.0	−21	8.9	1
3	45.07058	37.61042	Shugo MV, seepage 1	3-1/09BG	5.2	−31	10.3	1
4	45.02836	37.58561	Vostok MV, central seepage	15/09	3.3	−29	8.2	1
5	45.11867	36.89775	Bugaz MV, central seepage	4-1/09	10.1	−26	14.6	1
5	45.11867	36.89775	Bugaz MV, flank seepage	4-2/09	10.2	−28	15.0	1
5	45.11867	36.89775	Bugaz MV, eastern seepage	4-3/09	8.9	−27	13.5	1
7	45.20233	36.78258	Karabetova Gora MV, western seepage	1/09	14.2	−24	18.5	1
8	45.26925	36.96256	Shapur MV, central seepage	6-1/09	3.2	−33	8.6	1
9	45.18939	37.18353	Yuzhno-Neftyanoi MV, seepage with oil films	7/09	−3.2	−33	2.2	1
10	45.27808	37.38744	Miska MV, central seepage	10/09	1.2	−34	6.7	1
12	45.30942	37.03928	Tsymbaly-Vostok MV, seepage 1	17/09	2.9	−35	8.5	1
14	45.43231	36.92253	Kuchugur MV, central seepage	13-1/09	5.4	−22	9.4	1
15	45.35414	36.71381	Chushka MV, flank seepage	12-1/09	5.0	−33	10.4	1
15	45.35414	36.71381	Chushka MV, central seepage	12/09	3.0	−22	7.0	1
19	45.25181	37.43917	Gnilaya MV, central seepage near lake	9-2/09BG	1.5	−34	7.0	1
19	45.25181	37.43917	Gnilaya MV, southern group of seepages	9-3/09	0.9	−39	7.0	1
21	45.32461	37.17114	Sopka MV	11/09BG	−3.4	−35	2.2	1
South Caspian Province (see Fig. 3)								
Fore-Caspian area								
37	41.00317	49.19772	Zarat (Khydyrzyndy-2) MV	29/10	7.2	−25	11.6	2
47	41.15500	48.98386	Kaynardja MV	18/12	0.1	−28	4.9	1
Apsheron area								
3	40.46239	49.57422	Uchtepe MV	3/10	7.4	−21	11.3	2
12	40.25767	49.55056	Pelpelya-Garadag MV	10/10	3.1	−19	6.7	2
21	40.35197	49.55944	Shorbulag MV	17/10	2.1	−22	6.1	2
23	40.38189	49.58417	Davaboynu MV	19/10	3.2	−24	7.5	2
42	40.49294	49.70328	Cheildag MV	34/10	6.2	−13	9.1	2

(*Continued*)

MV No.	ºN lat.	ºE long.	Sampling site	Sample number*	VSMOW/ ‰			Data source***
					$\delta^{18}O$	δD	$\Delta\delta^{18}O$**	
Shemakha-Gobustan area								
1	40.48053	49.44811	Pirekyashkyul MV, northern group of seepages	1/10	3.1	−12	5.9	2
2	40.46625	49.46950	Pirekyashkyul MV, northern group of seepages	2/10	2.8	−21	6.7	2
4	39.99550	49.40642	Dashgil MV, central mud breccia field	4-1/10	2.0	−17	5.4	2
5	39.99561	49.40278	Dashgil MV, large seepage	4-2/10	2.5	−29	7.4	2
6	39.99861	49.47442	Bakhar MV	5/10	4.1	−26	8.6	2
7	40.00100	49.47031	Bakhar MV, northern group of seepages	5-1/10	2.5	−23	6.6	2
8	39.97019	49.34731	Saryboga MV, western group of seepages	6/10	3.2	−31	8.3	2
9	39.97358	49.35978	Goturdag MV	7/10	2.3	−31	7.4	2
10	39.99452	49.30911	Airantekyan MV	8/10	n.d.	n.d.	n.d.	2
22	40.31267	49.43722	Shakhigaya MV	18/10	1.9	−22	5.9	2
24	40.25078	49.24558	Galendarakhtarma MV	20/10	5.6	−14	8.6	2
25	40.35258	49.18122	Eastern Nardaran-Akhtarma MV	21/10	5.4	−15	8.5	2
26	40.82756	48.58558	Demirchi MV	22-1/10	10.4	−23	14.5	2
27	40.82756	48.58558	Demirchi MV	22-2/10	n.d.	n.d.	n.d.	2
28	40.51019	49.03208	Malyi Mereze MV	23/10	7.0	−21	10.9	2
31	40.29842	49.25425	Cheildag MV	26/10	4.9	−20	8.7	2
32	40.30089	49.26419	Cheildag MV, northern group of seepages	26-1/10	4.7	−12	7.5	2
33	40.30750	49.23358	Cheildag MV, western group of seepages	26-2/10	6.6	−14	9.6	2
34	40.30208	49.24000	Cheildag MV, southern group of seepages	26-3/10	5.4	−22	9.4	2
38	40.18611	49.23956	Gylych MV	30/10	4.8	−22	8.8	2
39	40.20617	49.21006	Agdam MV, group of seepages	31/10	2.7	−29	7.6	2
40	40.18083	49.18961	Arzani MV	32/10	5.1	−20	8.9	2
41	40.22075	49.16239	Shekikhan MV	33/10	8.2	−24	12.5	2
48	40.25131	48.84189	Kalamadyn MV, western group of seepage	1/12	4.8	n.d.	n.d.	1
49	40.30642	48.09720	Northern Inchabel MV	2/12	3.0	n.d.	n.d.	1
49	40.30642	48.09720	Northern Inchabel MV	3/13	1.3	−33	6.7	1
50	40.48044	49.03178	Shikhzarli MV	9/12	6.3	−27	10.9	1
45	40.81014	48.70581	Northern-Astrakhanka MV	10/12	10.3	−28	15.1	1

(*Continued*)

MV No.	ºN lat.	ºE long.	Sampling site	Sample number*	VSMOW/‰			Data source***
					$\delta^{18}O$	δD	$\Delta\delta^{18}O$**	
51	40.17442	48.96256	Kyrlyh MV	12/12	3.0	−20	6.8	1
52	40.08844	48.95444	Malyi-Kharami MV	13/12	1.7	n.d.	n.d.	1
53	40.43525	48.74017	Gushchu MV	15/12	1.0	−32	6.3	1
54	40.60908	48.56597	Matrasa MV	16/12	1.7	−26	6.2	1
55	40.21864	49.04072	Dashmardan MV, central seepage	19/12	5.4	−25	9.8	1
55	40.21914	49.04569	Dashmardan MV, flank seepage	19-1/12	3.6	−27	8.2	1
56	40.74378	48.43914	Baskal MV, northern group of seepages	20/12	2.8	−23	6.9	1
57	40.54942	49.30064	Weis MV	21/12	8.8	−20	12.6	1
58	40.52700	48.70000	Melikchoban MV	1/13	n.d.	n.d.	n.d.	1
59	40.58800	48.01000	Kelakhana MV	2/13	n.d.	n.d.	n.d.	1
60	40.52500	48.01800	Charkhan MV	4/13	n.d.	n.d.	n.d.	1
Fore-Kura area								
11	39.86128	49.29592	Khydyrly MV	9/10	1.0	−30	6.0	2
13	39.51211	49.10772	Duruvdag MV	11/10	1.2	−23	5.3	2
14	39.38161	49.14611	Duzdag MV, small seepage	12/10	2.0	−16	5.3	2
15	39.38161	49.14611	Duzdag MV, central seepage	12-1/10	3.3	−21	7.2	2
16	39.31475	49.18442	South-Neftechala MV	13/10	−0.6	−32	4.7	2
17	39.31833	49.18711	Oil well near South-Neftechala MV	13-1/10	n.d.	−32	n.d.	2
18	39.94703	49.07764	Malyi Mishovdag MV	14/10	2.3	−23	6.4	2
19	39.95308	49.05206	Bol'shoy Mishovdag MV	15/10	2.5	−16	5.8	2
20	39.88431	48.95014	Yandere MV	16/10	3.0	−18	6.5	2
29	39.92097	49.26481	Kalmaz MV	24/10	4.4	−16	7.7	2
35	40.19606	48.87050	Akhtarma-Pashaly MV	27/10	1.5	−21	5.4	2
43	39.70417	49.41172	Biandovan MV	35/10	3.7	−25	8.1	2
66	40.19036	48.90350	Bol'shoy Kharami MV, central seepage	14/12	2.7	−25	7.1	1
66	40.19030	48.90432	Bol'shoy Kharami MV, eastern group of seepages	14-2/12	2.4	−26	6.9	1

Notes: * Number after slash is year of sampling (specific number/year);
** $\Delta\delta^{18}O$ is shift from the Craig line of meteoric waters (Craig, 1961) was calculated as $\Delta\delta^{18}O = \delta^{18}O - (\delta D - 10)/8$;
*** Data source: 1 – this work; 2 – Lavrushin et al. (2015).
n.d. = no data.

Table 2 Chemistry of mud volcanic waters from the Caucasus region and the fluid generation temperatures based on Mg/Li geothermometry.

MV No.	Sample	T/°C	pH	TDS /(g·L^{-1})	Concentration /(g·L^{-1})			Concentration/ (mg·L^{-1})						CO_2/vol%	Mg/Li		Data source*
					HCO_3	Cl	Na	SO_4	K	Mg	Ca	Si	Li×1000		T/°C calc.	Depth/km	
Taman area of the Kerch-Taman Province																	
1	14-1/09	22.3	7.95	10.58	5.25	2.13	2.71	36.0	19.9	27.6	13.7	4.85	1.21	17.4	87	2.18	1, 2
1	14-3/09	23.0	8.25	11.47	5.61	2.13	3.01	176.1	16.3	27.9	8.1	5.34	1.16	8.0	86	2.15	1, 2
2	2/09BG	n.d.	6.93	20.07	0.61	11.35	5.84	1.5	229.6	114.9	1560.0	6.68	13.26	1.7	136	3.40	1, 2
3	3-1/09BG	21.0	7.76	18.03	3.54	7.80	5.73	119.8	65.9	77.2	29.8	18.2	11.18	4.5	137	3.43	1, 2
4	15/09	n.d.	8.67	10.87	3.90	3.19	3.01	353.4	41.1	42.7	15.9	6.69	0.54	6.9	63	1.57	1, 2
5	4-1/09	20.0	7.94	13.34	6.22	2.62	3.83	35.5	79.7	101.8	24.6	17.7	2.00	6.4	83	2.08	1, 2
5	4-2/09	23.2	8.27	15.02	6.83	3.05	4.41	64.4	55.6	107.9	19.7	24.1	1.83	n.d.	80	2.01	1, 2
5	4-3/09	n.d.	8.00	14.30	6.10	3.19	4.41	30.7	36.4	78.3	10.2	16.0	1.58	n.d.	81	2.02	1, 2
7	1/09	17.9	8.02	15.44	9.25	1.46	3.82	23.9	55.2	63.2	21.0	9.65	1.97	22.0	89	2.23	1, 2
8	6-1/09	21.6	7.73	18.42	4.27	5.74	8.01	61.3	30.0	53.2	14.6	3.91	1.09	n.d.	76	1.91	1, 2
9	7/09	30.3	6.60	0.80	0.37	0.14	0.11	26.9	9.3	7.3	114.2	9.67	0.02	5.3	18	0.46	1, 2
10	10/09	n.d.	7.81	12.09	2.39	5.29	4.30	46.1	14.0	31.6	22.0	5.07	0.22	1.9	47	1.18	1, 2
12	17/09	25.0	n.d.	11.87	3.29	4.47	3.90	11.8	30.8	34.0	30.9	6.36	1.08	n.d.	82	2.05	1, 2
14	13-1/09	n.d.	6.98	16.05	3.78	4.96	4.81	1462.1	29.6	115.9	173.1	12.8	1.02	16.9	66	1.65	1, 2
15	12/09	17.8	7.82	11.63	3.05	4.26	4.12	8.4	30.9	33.3	30.5	6.09	1.07	3.7	82	2.04	1, 2
15	12-1/09	18.2	7.81	10.96	3.90	3.26	3.60	n.d.	25.3	35.6	34.5	8.82	0.84	5.3	75	1.87	1, 2
19	9-2/09BG	n.d.	8.79	13.10	2.44	5.82	4.60	24.0	5.8	13.3	4.6	2.74	0.11	0.8	41	1.02	1, 2
19	9-3/09	n.d.	8.66	13.12	2.56	5.53	4.75	48.3	6.1	5.8	3.3	4.39	0.12	0.5	51	1.28	1, 2
21	11/09BG	25.5	8.84	9.59	1.83	3.05	2.90	1200.6	12.8	10.9	9.7	2.98	0.20	6.7	56	1.41	1, 2
Fore-Caspian area of the South Caspian Province																	
37	29/10	13.1	7.42	35.3	2.04	21.56	10.92	14.3	186.4	123.4	123.0	6.62	14.08	2.4	137	6.52	1, 3
47	18/12	17.4	6.69	63.8	0.89	37.59	23.22	n.d.	94.9	654.8	813.4	2.68	3.61	5.6	75	3.57	1
Apsheron area of the South Caspian Province																	
3	3/10	18.9	7.77	10.7	5.06	2.41	2.92	10.1	8.3	28.3	15.3	6.83	0.69	1.1	73	3.48	1, 3
12	10/10	n.d.	8.65	20.5	5.80	7.66	6.56	59.7	7.8	66.9	18.8	2.01	0.59	0.2	60	2.85	1, 3
21	17/10	14.2	7.82	13.2	1.37	5.82	4.38	961.9	15.8	75.3	107	3.52	0.36	1.5	48	2.29	1, 3
23	19/10	15.6	7.65	19.4	1.36	10.78	6.73	13.5	25.3	214.8	94.0	7.58	1.30	2.2	64	3.06	1, 3
42	34/10	13.7	8.27	9.6	2.53	3.17	2.98	7.7	11.1	11.5	8.5	3.96	0.38	0.6	70	3.32	1, 3

(*Continued*)

MV No.	Sample	T/°C	pH	TDS /(g·L^{-1})	Concentration /(g·L^{-1})			Concentration/ (mg·L^{-1})						CO_2/vol%	Mg/Li		Data source*
					HCO_3	Cl	Na	SO_4	K	Mg	Ca	Si	Li×1000		T/°C calc.	Depth/km	
Shemakha-Gobustan area of the South Caspian Province																	
1	1/10	15.0	8.00	18.7	8.10	3.98	5.67	454.5	20.9	81.3	13.0	6.09	0.87	2.9	66	3.16	1, 3
2	2/10	16.0	8.00	13.2	6.07	2.46	3.80	13.4	13.3	37.3	6.3	10.2	0.77	4.0	73	3.46	1, 3
4	4-1/10	19.0	7.45	24.0	0.49	12.74	7.50	9.3	17.2	362.3	217	4.51	0.46	1.0	37	1.78	1, 3
5	4-2/10	19.6	7.49	38.2	1.76	15.89	11.70	3168.1	24.0	351.6	83.2	4.48	1.17	2.2	57	2.69	1, 3
6	5/10	20.0	7.84	14.7	2.47	6.07	4.83	29.3	10.8	14.0	13.2	4.39	0.41	2.5	69	3.30	1, 3
7	5-1/10	19.0	7.92	34.7	2.50	16.89	11.78	466.0	18.4	159.0	18.2	3.15	0.24	0.9	33	1.57	1, 3
8	6/10	18.5	7.88	14.5	1.40	7.55	5.27	5.1	9.7	65.3	25.0	5.82	0.39	0.6	51	2.43	1, 3
9	7/10	19.6	7.58	18.4	4.15	6.48	5.55	84.7	15.4	111.0	31.7	6.80	0.90	0.8	63	3.02	1, 3
10	8/10	17.5	7.58	18.1	3.23	7.47	5.91	236.4	11.8	119.9	29.0	5.77	0.49	3.0	50	2.37	1, 3
22	18/10	14.7	7.60	34.0	0.57	15.37	9.41	553.0	9.3	392.3	244	4.58	0.21	0.3	23	1.07	1, 3
24	20/10	13.9	7.99	15.2	7.02	2.49	4.23	72.2	7.1	25.4	6.3	4.17	0.78	3.2	77	3.69	1, 3
25	21/10	13.0	7.52	16.3	5.30	4.26	4.86	650.1	15.3	80.3	43.7	7.76	0.67	4.3	60	2.88	1, 3
26	22-1/10	10.0	8.02	8.6	3.97	1.41	2.38	67.0	9.4	22.8	9.2	4.71	2.00	3.6	103	4.91	1, 3
27	22-2/10	9.0	7.60	8.6	4.24	1.27	2.36	3.4	17.9	18.1	13.8	5.59	2.78	3.5	116	5.53	1, 3
28	23/10	11.1	7.98	10.0	3.08	3.27	3.23	59.6	8.8	31.8	11.3	4.88	0.26	1.2	50	2.38	1, 3
31	26/10	16.1	8.46	13.4	5.72	3.08	4.03	31.7	18.1	59.1	10.6	4.76	1.68	2.0	86	4.09	1, 3
32	26-1/10	15.4	8.12	12.5	6.01	1.91	3.35	2.5	18.0	65.2	14.1	2.65	0.98	2.0	71	3.40	1, 3
33	26-2/10	14.5	7.82	10.6	4.15	2.31	3.01	68.8	10.8	32.7	9.5	6.45	0.96	3.6	79	3.77	1, 3
34	26-3/10	14.8	7.82	11.8	4.54	3.07	3.62	45.7	28.0	37.9	18.3	6.79	1.88	4.7	95	4.50	1, 3
38	30/10	15.9	7.48	17.5	5.26	5.78	5.45	6.4	39.6	107.9	49.8	10.8	2.58	10.4	89	4.25	1, 3
39	31/10	14.8	8.10	22.9	5.14	8.02	6.97	187.4	24.5	113.3	15.8	4.99	0.17	1.8	29	1.40	1, 3
40	32/10	16.8	7.66	15.7	5.73	4.22	4.74	8.6	33.0	64.6	19.8	14.7	2.19	6.5	92	4.36	1, 3
41	33/10	14.4	8.00	9.9	3.72	2.54	2.97	128.1	21.0	43.5	42.3	4.73	0.55	2.3	63	3.00	1, 3
48	1/12	18.5	8.05	13.9	1.15	7.17	4.91	21.1	12.0	81.9	19.0	2.88	0.07	1.3	18	0.84	1
49	2/12	18.0	7.37	16.8	0.85	8.92	5.84	3.1	24.4	63.8	112	8.23	0.48	2.2	56	2.66	1
49	3/13	n.d.	8.50	15.0	2.07	5.74	4.56	734.4	22.3	131.7	25.0	4.41	0.07	0.8	12	0.59	1
50	9/12	14.0	7.99	8.8	3.26	1.31	2.33	628.7	12.0	19.8	9.5	5.96	0.28	2.2	57	2.70	1
50	5/13	n.d.	8.10	8.6	4.17	1.31	2.38	27.5	11.0	15.5	13.1	4.89	1.52	8.6	101	4.81	1
45	10/12	12.6	8.02	9.0	4.92	0.70	2.29	2.5	17.1	4.6	2.0	6.52	0.49	3.8	87	4.14	1

(*Continued*)

MV No.	Sample	T/°C	pH	TDS /(g·L^{-1})	Concentration /(g·L^{-1})			Concentration/ (mg·L^{-1})						CO_2/vol%	Mg/Li		Data source*
					HCO_3	Cl	Na	SO_4	K	Mg	Ca	Si	Li×1000		T/°C calc.	Depth/km	
51	12/12	20.8	7.88	26.2	1.74	14.97	10.00	2.7	8.7	174.0	15.4	5.51	0.39	3.6	41	1.96	1
52	13/12	18.5	7.58	25.1	0.85	14.38	9.43	2.7	25.6	67.7	59.6	3.74	0.27	2.2	43	2.05	1
53	15/12	18.3	7.46	20.4	0.99	10.74	7.06	7.5	36.9	90.1	74.1	4.58	1.21	3.2	73	3.46	1
54	16/12	23.8	7.56	24.0	5.63	10.28	8.47	5.3	34.0	139.1	27.1	7.16	1.99	9.7	79	3.78	1
55	19/12	n.d.	7.76	11.9	2.70	3.28	3.30	463.4	15.0	20.5	21.3	10.0	0.63	n.d.	75	3.56	1
55	19-1/12	17.5	7.35	11.8	2.65	4.16	3.72	378.5	13.6	42.0	62.4	9.55	0.37	5.8	55	2.62	1
56	20/12	17.4	7.63	7.6	0.40	2.09	1.67	508.9	11.8	15.1	31.9	5.28	0.67	1.7	80	3.81	1
57	21/12	20.9	7.96	11.5	5.82	1.53	3.17	103.6	21.0	21.7	14.3	11.8	0.46	3.6	67	3.18	1
58	1/13	n.d.	8.20	6.7	0.71	3.49	2.50	31.1	11.1	9.0	18.6	4.74	0.25	0.5	63	3.01	1
59	2/13	n.d.	8.10	12.7	4.92	2.27	3.17	6.9	31.2	63.2	19.2	9.28	1.55	4.4	83	3.95	1
60	4/13	n.d.	7.80	17.7	2.99	7.35	5.25	5.4	46.2	251.1	125.7	21.1	1.37	5.9	64	3.04	1
Fore-Kura area																	
11	9/10	17.9	7.47	28.3	0.11	16.17	8.78	9.0	15.6	259.2	1085.4	2.70	0.19	2.9	24	1.60	1, 3
13	11/10	19.9	7.89	37.1	1.36	19.92	13.23	13.0	16.2	84.0	20.3	3.97	0.03	0.5	n.d.	n.d.	1, 3
14	12/10	20.3	7.61	47.3	1.10	20.40	13.21	3.3	18.2	170.2	82.1	6.36	0.12	0.5	21	1.39	1, 3
15	12-1/10	n.d.	7.41	25.6	1.13	12.81	8.59	6.6	15.2	41.2	43.0	9.45	0.17	0.6	39	2.59	1, 3
16	13/10	19.0	6.51	84.3	0.41	46.07	24.29	12.6	73.5	981.0	3326.2	14.6	1.20	3.5	47	3.10	1, 3
17	13-1/10	22.6	n.d.	40.4	0.12	24.60	13.71	8.0	40.1	465.3	1195.3	11.3	0.61	3.4	41	2.71	1, 3
18	14/10	17.5	7.46	20.3	3.25	8.30	6.28	n.d.	22.3	145.2	36.1	6.27	0.59	2.0	51	3.42	1, 3
19	15/10	16.0	7.60	14.6	2.14	6.48	4.79	6.1	16.6	92.3	31.2	4.23	0.16	0.5	30	2.03	1, 3
20	16/10	17.5	7.69	12.2	1.02	5.99	4.05	n.d.	10.2	86.0	43.1	5.95	0.13	1.2	27	1.83	1, 3
29	24/10	16.0	7.97	16.6	2.26	7.61	5.62	26.0	11.6	66.7	37.0	6.73	0.49	9.5	56	3.70	1, 3
35	27/10	15.5	7.29	16.8	3.54	6.62	4.78	n.d.	18.0	359.5	133.2	18.4	0.66	1.6	45	2.97	1, 3
43	35/10	15.5	7.76	25.1	1.25	11.10	7.42	n.d.	19.5	78.4	72.7	4.62	0.54	3.3	56	3.73	1, 3
66	14/12	18.7	8.00	18.4	2.11	8.68	6.32	3.7	13.2	40.7	11.1	5.26	0.10	2.7	29	1.90	1, 3
66	14-2/12	n.d.	8.09	24.3	3.43	9.55	7.40	17.5	13.5	38.1	5.0	4.52	0.06	3.5	21	1.39	1, 3

Notes: Sampling sites numbers are same as in Table 1.
TDS = Total Dissolved Solids;
* Data source: 1 – this work; 2 – Kikvadze et al. (2014) with original extra data (1) on SO_4, K, Ca, and Si contents in MV waters and CO_2 content in gas phase; 3 – Lavrushin et al. (2015) with original extra data (1) on CO_2 content in gas phase.
n.d. = no data

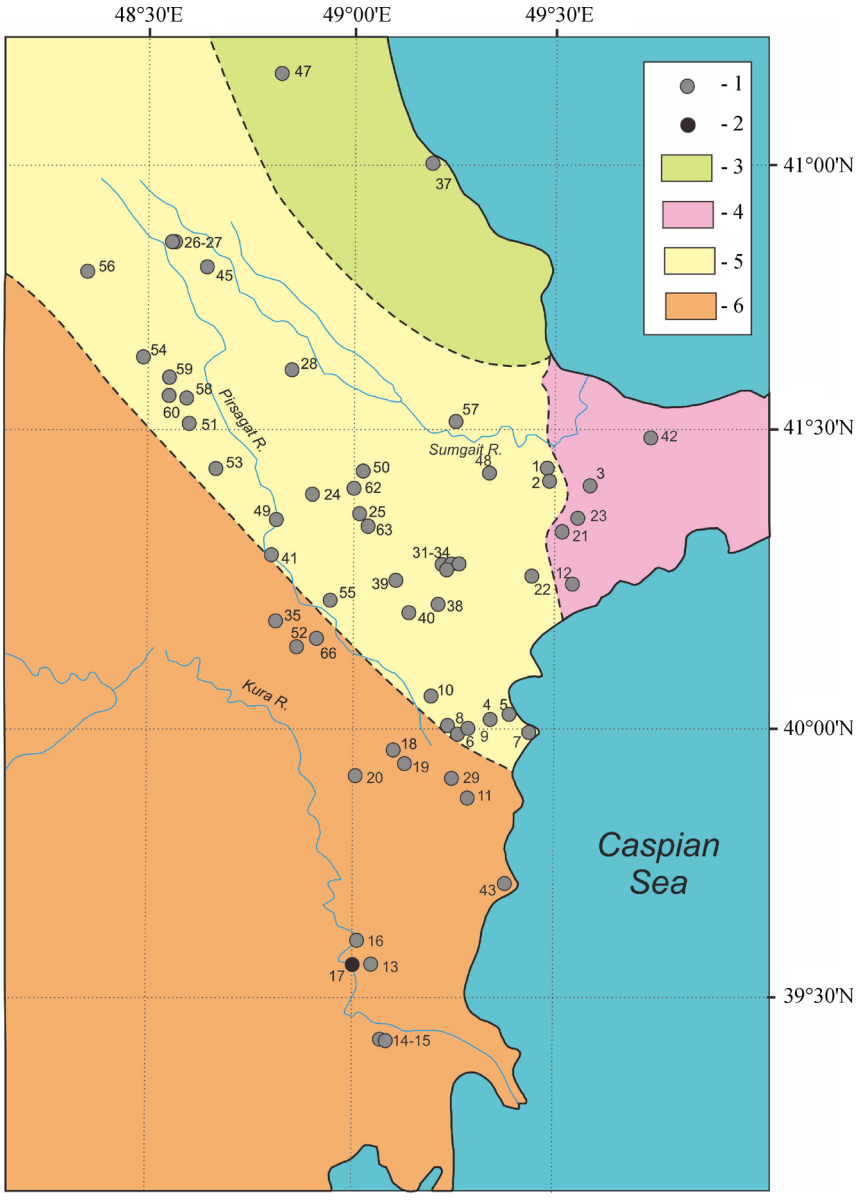

Fig. 3 Location map of mud volcanoes in the South Caspian MV province, Azerbaijan. 1 – mud volcanoes; 2 – Neftechala oil well; 3-6 – petroleum areas: Fore-Caspian (3), Apsheron (4), Shemakha-Gobustan (5), ForeKura (6), according to (Jakubov et al., 1971). Sampling sites numbers are same as in Table 1.

The bulk chemistry of MV gases was analyzed on a *Crystal-2000 M* gas chromatography analyzer at the Geological Institute (GIN, Moscow, Russia), by absolute calibration of each component against standard gas mixtures. Carbon dioxide was determined on a flame-ionization detector with a built-in methanizer. The error was within 0.5 vol.% for each component.

Fluid generation temperatures were estimated using an Mg–Li geothermometer designed originally (Kharaka and Mariner, 1989) for low to high saline pore and edge waters in oil and gas basins, with temperatures up to 300°C:

$$T_{Mg/Li}\ (°C) = 2200/(\lg((\sqrt{Mg})/Li) + 5.47) - 273.15.$$

The Mg-Li thermometer is less sensitive to water salinity and aquifer lithology and the most suitable for basinal waters (Kharaka and Mariner, 1989); it provides more reliable estimates than its SiO_2, K-Na, Na-Li and K-Na-Ca counterparts (Lavrushin et al., 2003).

4 Results

4.1 Chemistry of MV free gas

The gas phase of MVFs in the Caucasus region contains ~70 vol.% to 99 vol.% CH_4, a few percent to 30 vol.%

CO_2, and vanishing amounts of heavy CH gases ($<<$ 0.5 vol.% ethane, $<<$ 0.005 vol.% propane, etc.) (Kikvadze et al., 2014; Lavrushin et al., 2015). Average carbon dioxide contents are 7.2 vol.%, 5.3 vol.%, and 4.3 vol.% in the Taman Peninsula, in the South Caspian province, and in the Kakhety area, respectively, but is often much lower or even below detection limit. The highest CO_2 contents reaching ~30 vol.% were measured in gas released from Kuchugur volcano in the Taman Peninsula, where CO_2 content in MVFs generally increases toward the Kerch strait. The gas phase composition correlates with the mud volcanic activity in both the Taman and Azerbaijan provinces. The concentration of CO_2 in MV gases is commonly high in central most active high-rate issues but lower on the periphery. Nitrogen is most often $<$ 1 vol.% and rarely reaches 5.4 vol.% in the MV gases, whereas inert gases and hydrogen occur as impurities (Kikvadze et al., 2014, Lavrushin et al., 2015).

4.2 Chemistry of MV water

MV waters in both Taman and South Caspian provinces are Na^-, Cl^- and HCO_3^- dominated with lesser amounts of Mg^+ and Ca^{2+} (Fig. 4). The Taman MV waters have HCO_3-Cl/Na and Cl-HCO_3/Na compositions with high contents of HCO_3^- while the South Caspian waters are mainly of Cl/Na and Cl-HCO_3/Na types. Commonly the waters that emanate CO_2-rich gases are also enriched in HCO_3^- (Fig. 5), i.e., HCO_3^- concentrations correlate with the gas phase composition. Generally the HCO_3^- concentrations in the Taman MVFs increase progressively west- and south-westward, along with CO_2 increase in the gas phase.

Waters released from the Taman MVs differ from those in the South Caspian province in TDS ranges: 9.6 to 20.1 g/L and 8.6 to 63.8 g/L, respectively (Table 2). This may reflect the original difference between the compositions of pore waters in the Indol-Kuban Trough and the Lower Kura basin. On the other hand, salinity of the greatest part of pore water samples in both MV provinces may be as low as 20 g/L (Table 2), possibly, due to freshening by waters from hydrocarbon reservoirs or due to smectite dehydration at depths.

4.3 Oxygen and hydrogen isotope compositions of H_2O

The oxygen and hydrogen isotope compositions of MV waters are largely similar in MVFs from different Caucasian provinces (Fig. 6) and different from those of local surface (stream), marine, and pore waters, and especially, CO_2-rich springs in Northern Caucasus (Lavrushin, 2012; Dubinina, 2013). The Northern Caucasus CO_2-rich mineral springs also differ from MVFs in low salinity (Table 2), which is below 2.5 g/L in 94 (out of 172)

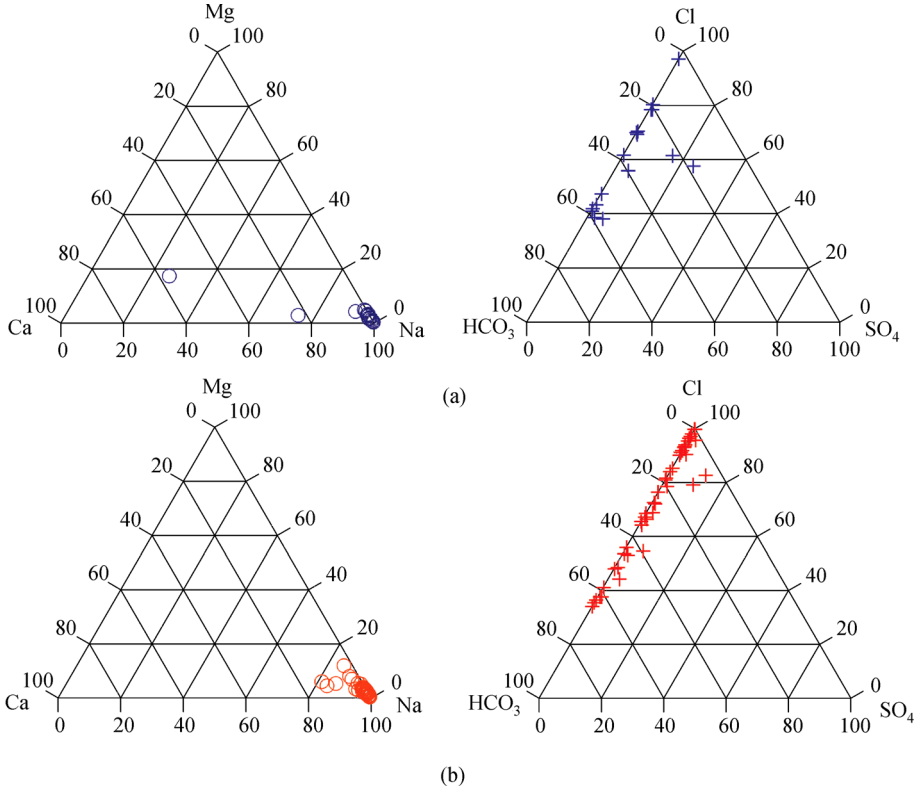

Fig. 4 Major ions composition of mud volcanic waters from different Caucasian MV provinces (mg-equ %). (a) Kerch-Taman province, (b) South Caspian province.

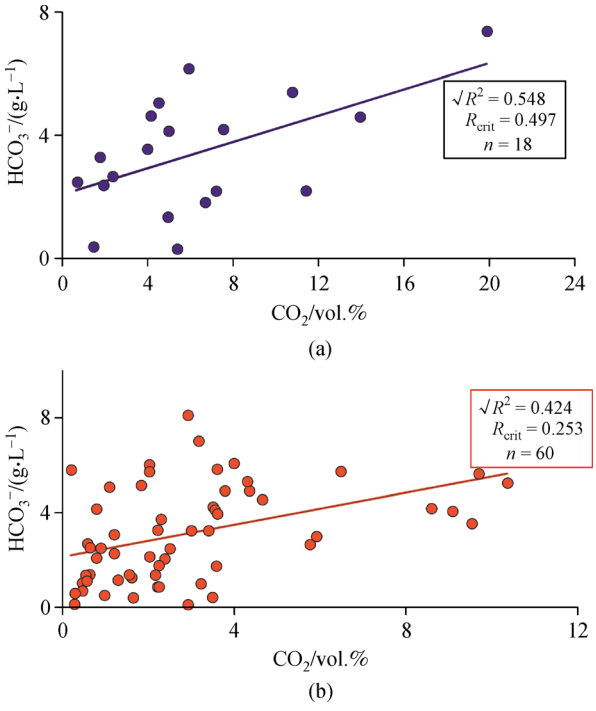

Fig. 5 Correlation of CO_2 (vol.%) in free gases and HCO_3^- (g/L) in MV waters from the Caucasian MV provinces. (a) Kerch-Taman province, (b) South Caspian province. Straight lines are statistically significant correlation trends.

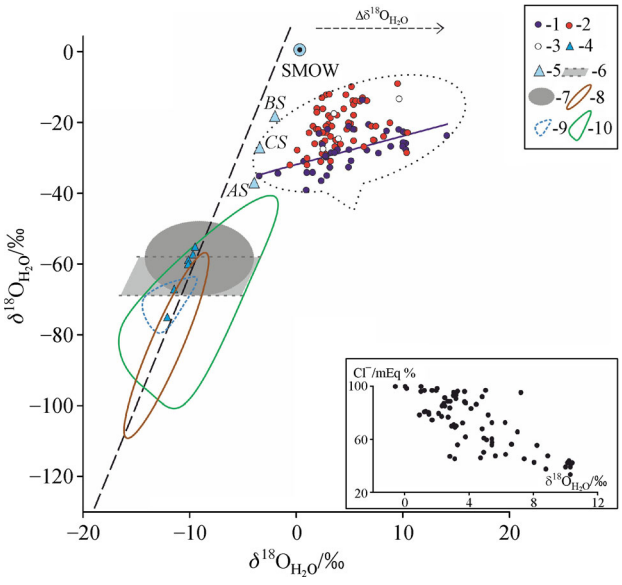

Fig. 6 Oxygen and hydrogen isotope compositions of water from the Caucasus region. 1-3 – MV waters of the Kerch-Taman (1), South Caspian (2), and Kakhety (3) provinces; 4 – fresh water, 5 – sea water, after (Dubinin and Dubinina, 2014) (AS = Sea of Azov, CS = Caspian Sea, BS = Black Sea), 6-7 – pore waters from hydrocarbon reservoirs, after (Seletskii, 1991), Azov-Kuban basin (6) Neftechala oil field in the South Caspian basin (7); 8 – CO_2-rich springs from the Elbrus area; 9 – CO_2-rich springs from West Caucasus; 10 – boreholes from the North Caucasus (8-10 – after Seletskii, 1998; Lavrushin, 2012; Dubinina, 2013). Dash line is Craig line of meteoric water composition (Craig, 1961). Solid line is statistically significant correlation trend inferred from the Taman MVs data. Black dots in inset are all data set on MV waters from the Caucasus region.

samples and below 5.0 g/L in 43 other samples (Lavrushin, 2012) while MVFs in different Caucasian provinces contain 13.3 to 22.4 g/L TDS on average.

The $\delta^{18}O$–δD compositions of MVFs from all Caucasian provinces (Fig. 6) fall to the right of the Craig line for meteoric waters (Craig, 1961 and 1963). The maximum $\delta^{18}O_{H_2O}$ values for MV waters from each province are much higher than in the meteoric endmember which is apparently about −5 ‰ in the region (Lavrushin et al., 2005; Dubinina et al., 2005; Lavrushin, 2012).

Thus, the $\delta^{18}O$ and δD values in all studied water samples suggests the same formation mechanism for MV waters all over the Caucasian region. In the δD–$\delta^{18}O$ diagram, the modern oceanic water (SMOW), with $\delta^{18}O_{H_2O} = 0 \pm 1$ ‰ (at 19.35 g/L Cl^- and 0.14 g/L HCO_3^-) (Horn, 1969), plots much above the composition field of the Taman MV waters. The intersection of the Taman MVF trend with the Craig line, in its turn, lies high above the trends for both meteoric surface waters and pore waters in the Azov-Kuban and Kura oil and gas basins, which have similar δD and $\delta^{18}O$ compositions (Table 3). Many data points of CO_2-rich springs from the central (Elbrus-Kazbek) and western segments of the Greater Caucasus, as well as waters from boreholes, lie farther below the δD and $\delta^{18}O$ fields of pore waters from hydrocarbon reservoirs (Lavrushin, 2012; Dubinina, 2013).

The oxygen isotopic shift ($\Delta\delta^{18}O_{H_2O}$) is a "stagnation" criterion for pore waters or, in a more general case, an indicator of the formation depth of groundwater (Ferronsky and Polyakov, 2012). Higher $\delta^{18}O_{H_2O}$ in the Caucasian MV fluids hardly can result from greater inputs of evaporitic brines, as we obtained the lowest $\delta^{18}O_{H_2O}$ for the most saline samples (Tables 1 and 2). Note that $\delta^{18}O_{H_2O}$ is in negative correlation with Cl^- (Fig. 6). The $\delta^{18}O$ and δD of MVFs bear strong impacts of dehydration waters released during illitization of smectite (Revil, 2002; Dählmann and de Lange, 2003; Lavrushin et al., 2005; Chelnokov et al., 2018; Sokol et al., 2019).

5 Discussion

5.1 Mud volcanic waters: major-ion chemistry and stable isotope composition

In spite of considerable geographic variations, the chemistry of MV waters worldwide shows distinct correlations with tectonic settings (Dimitrov, 2002; Kopf, 2002; Oppo et al., 2014; Kokh et al., 2015; Ershov and Levin, 2016; Mazzini and Etiope, 2017; Sokol et al., 2019). Mud volcanoes within the tectonically active

Table 3 Oxygen and hydrogen isotope compositions of MV water in comparison with pore water, sea water and spring water (the Caucasus region)

Water variety, provinces	VSMOW/ ‰		Data source*
	δD	δ^{18}O	
MV water, Kerch-Taman province	−39.0 – −21.0 −29.2 ± 2.5 (n = 18)	−3.4 – + 14.2 + 5.4 ± 2.0 (n = 18)	1
MV water, South Caspian province	−33.0 – −12.0 −22.6 ± 1.5 (n = 51)	−0.6 – + 10.4 + 3.9 ± 0.7 (n = 53)	1, 2
Fore-Caspian area	−28.0 – −25.0 −26.5 (n = 2)	+ 0.1 – + 7.2 + 3.7 (n = 2)	1, 2
Apsheron area	−24.0 – −13.0 −19.8 ± 3.7 (n = 5)	+ 2.1 – + 7.4 + 4.4 ± 2.0 (n = 5)	1, 2
Shemakha-Gobustan area	−33.0 – −12.0 −22.5 ± 2.0 (n = 31)	+ 1.0 – + 10.4 + 4.5± 0.8 (n = 33)	1, 2
Fore-Kura area	−32.0 – −16.0 −22.5 ± 2.8 (n = 13)	−0.6 – + 4.4 + 2.3 ± 0.7 (n = 13)	1, 2
MV water, Kakhety province	−1.0 – −27.0 −16.3 ± 9.0 (n = 5)	+ 2.0 – + 9.6 + 4.3 ± 2.7 (n = 5)	3
Pore water (Neftechala oil field)	−73.0 – -49.0 −55.0 ± 4.9 (n = 20)	−11.7 – -2.4 −6.0 ± 1.1 (n = 20)	4
Pore water (oil and gas reservoirs of the Azov-Kuban Basin)	−68.0 – -58.0	n.d.	5
Fresh meteoric waters, South Caspian province	−67.0 – −55.0 −59.0 ± 4.0 (n = 5)	−11.5 – −9.6 −10.3 ± 0.6 (n = 5)	2
Sea water (Sea of Azov)	−42.0	−3.4	4
Sea water (Black Sea)	−18 – −25 −21.5 (n = 2)	−4 – −3 −3.5 (n = 2)	4
Sea water (Caspian Sea)	−27.0	−3.0	2

* Notes: 1 – this work; 2 – Lavrushin et al. (2015); 3 – Lavrushin et al. (2012); 4 – Seletskii (1991); 5 – Vetshtei`n (1982); 6 – Kikvadze et al. (2014).
n.d. = no data.

circum-Pacific belt release several types of waters: HCO_3-Cl/Na, Cl-HCO_3/Na, and Cl/Na, with high concentrations of HCO_3^-, especially, in Sakhalin Island where average salinity reaches 15–16 g/L (Lagunova and Gemp, 1978; Ershov et al., 2016; Chelnokov et al., 2018), and in Taiwan Island (Gieskes et al., 1992; You et al., 2004). Generally, the HCO_3-Cl/Na and Cl-HCO_3/Na-type waters become more saline as HCO_3^- increases. The MV waters of Cl/Na type show large salinity ranges and most often occur in the Alpine-Himalayan belt. Their salinity reaches almost the highest brine values (25–50 g/L) within the influence zone of the Great Caucasus orogeny (Georgia and Azerbaijan), as well as on the eastern extension of the South Caspian MV province (Turkmenistan). Unlike these, the waters of the Kerch-Taman MV province in the area of decaying orogeny mainly have Cl-HCO_3/Na chemistry and a lower salinity of ~14 g/L (Lagunova and Gemp, 1971 and 1978; Dimitrov, 2002; Kopf, 2002 and 2003; Lavrushin et al., 2003; Kokh et al., 2015; Olenchenko et al., 2015; Ershov and Levin, 2016; Sokol et al., 2019).

The new data set from the Great Caucasus orogeny zone fits well this general pattern and provides a more detailed picture. The distribution of main MV water types (Cl/Na, Cl-HCO_3/Na, and HCO_3-Cl/Na) is random in the Taman and Kakhety areas but more regular in the South Caspian province. Specifically, waters are mostly of Cl/Na type in the Fore-Kura petroleum province but mainly have HCO_3-Cl/Na or Cl-HCO_3/Na compositions in the Shemakha-Gobustan and Apsheron areas. The HCO_3/Na-type MV waters tend to the tectonically active Greater Caucasus frontal zone of continental collision (Lavrushin et al., 2015). They are mainly restricted to the southern slope of the Greater Caucasus, while the Cl-type MV waters are more common to the Kura and Caspian basins which are filled with thick sediments (Fig. 7) and less stressed tectonically (Guliev et al., 2002; Reilinger et al., 2006; Aliev and Bairamov, 2007; Lavrushin et al., 2015).

Note that the chemically different waters differ also in δ^{18}O and $T_{Mg/Li}$: these values are generally higher in HCO_3-rich waters than in those of the Cl/Na type (Table 2). The Azerbaijan MVs discharging mainly HCO_3-Cl/Na waters are located in active tectonic and seismic zones around the southern slope of the Great Caucasus Range (Fig. 7), where plate velocities decrease dramatically to 4 mm/yr from ~13 mm/yr in the Kura basin (Mosar et al., 2010; Kadirov et al., 2015).

Judging by $T_{Mg/Li}$ values (Table 2), HCO_3-rich MV waters form at higher temperatures than those of Cl/Na-type, either due to higher temperature gradients in active areas or because hotter waters from deeper aquifers can rise

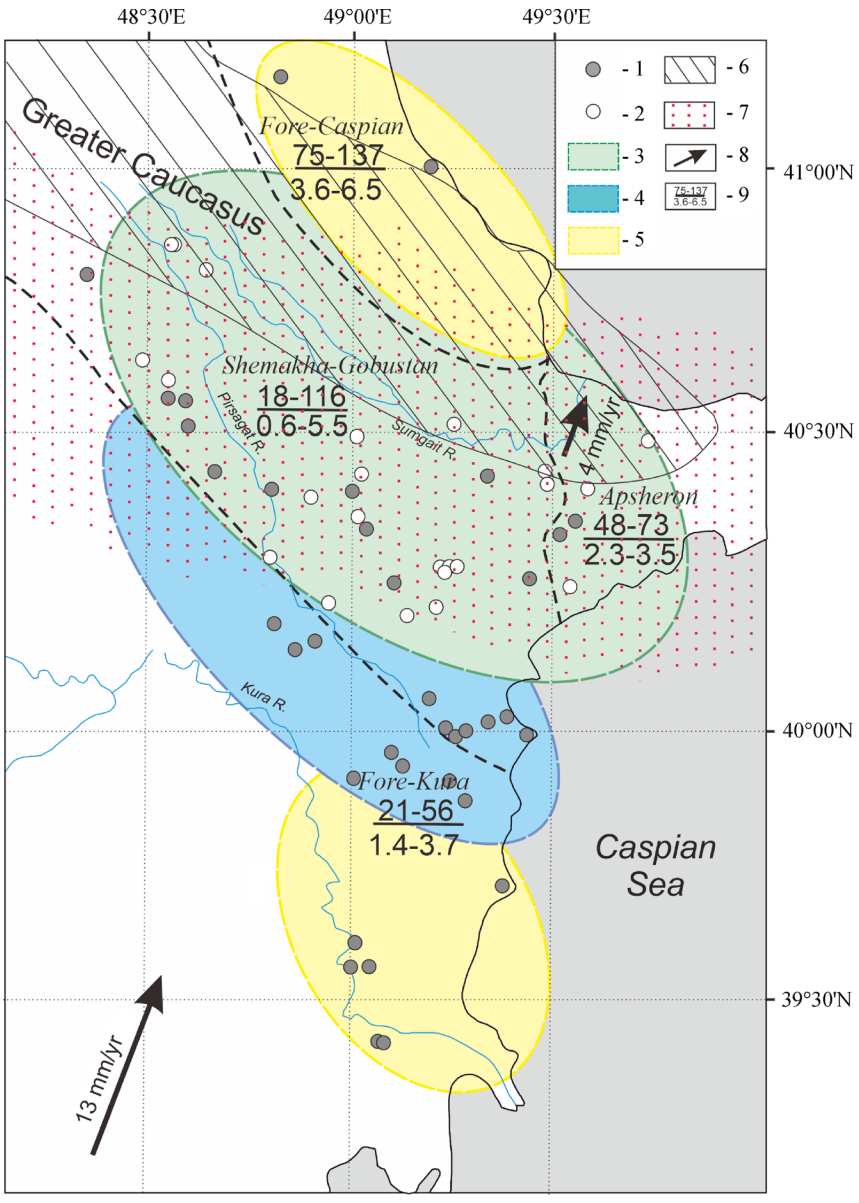

Fig. 7 Constrained MV fluid generation temperatures ($T_{Mg/Li}$) and depths ($H_{Mg/Li}$) of mud volcanic reservoirs within the South Caspian province. Dash lines – the boundaries of MV areas. 1 – MV waters with $HCO_3^- < 25$ mg-equ %, 2 – MV waters with $HCO_3^- > 25$ mg-equ %; 3-5 – distribution areas of different MV water types: 3 – HCO_3-Cl/Na type, 4 – Cl-HCO_3/Na type, 5 – Cl/Na type; 6 – the Great Caucasus, 7 – zone of high seismicity (Kadirov et al., 2012), 8 – general thrust direction after Reilinger et al. (2006) and Mosar et al. (2010), 9 – ranges of estimated $T_{Mg/Li}$ and $H_{Mg/Li}$ values. The specific values see in Table 4.

to the surface through faulted crust.

The Cl/Na MV waters of the Fore-Kura area and the Cl-HCO_3/Na and HCO_3-Cl/Na MV waters of the Shemakha-Gobustan and Apsheron areas differ markedly in oxygen isotope composition. The former (Table 1) have high salinity (25 to 84 g/L) and relatively low $\delta^{18}O_{H_2O}$ ($\leqslant +4.4$ ‰) while the latter (Tables 1 and 2) are less saline (10–20 g/L) but isotopically heavier, with up to + 10.4 ‰ $\delta^{18}O(H_2O)$. The heavier MV waters with high ^{18}O and HCO_3^- contents may result partly from dehydration of marine shale during sediment maturation and compaction at temperatures up to 200°C (Seletskii, 1991; Giggenbach, 1995; Lavrushin et al., 1996; Dählmann, and de Lange, 2003; Chelnokov et al., 2018). The percentages of dehydration water in MVFs from different Caucasian provinces, estimated after Chelnokov et al. (2018), are approximately 20% to 80% in Kerch (Sokol et al., 2019), 20%–60% in Taman, 20% to 55% in Shemakha-Gobustan, 25% to 50% in Apsheron, and as low as 10% to 35% in the Fore-Kura area (Table 3). A zone of rapid smectite illitization and dehydration was detected in the 7–13 km depth interval by seismic surveys in the South Caspian

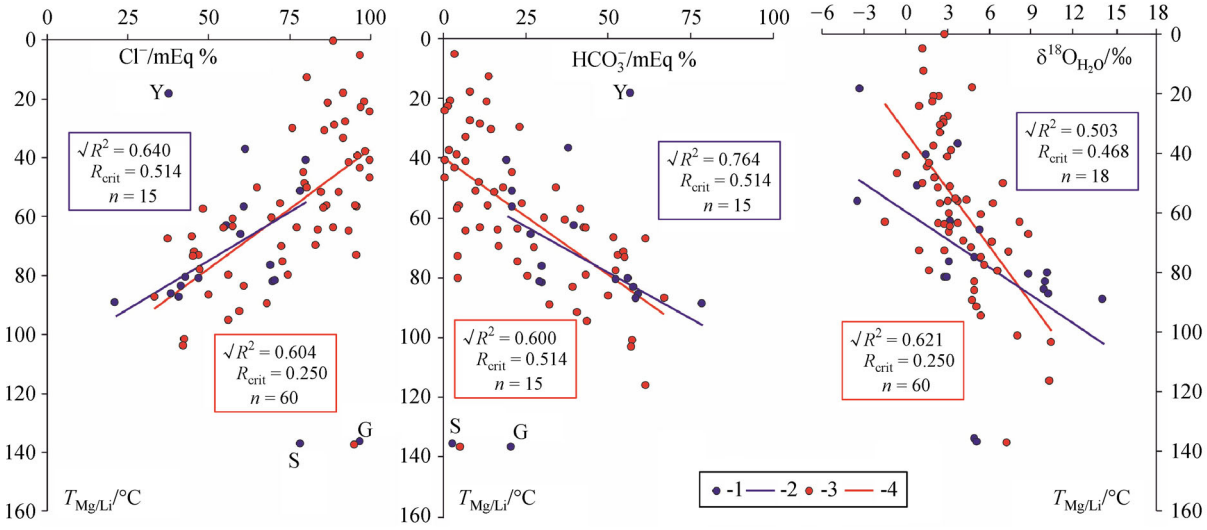

Fig. 8 Correlation of calculated $T_{Mg/Li}$(°C), Cl^- and HCO_3^- contents, and $\delta^{18}O_{H_2O}$ values in MV fluids. 1, 2 and 3, 4 are data points (1, 3) and trend (2, 4) in the Kerch-Taman and South Caspian provinces, respectively. Letters S, G and Y mark anomalous data points at Shugo, Gladkov, and Yuzhno-Neftyanoi mud volcanoes (Numbers 2, 3 and 9 in Tables 1 and 2, respectively).

region (Guliev et al., 1988).

The Cl^- and HCO_3^- contents, as well as $\delta^{18}O_{H_2O}$ and δD_{H_2O} values, of the Caucasian MVFs correlate well with the constrained temperatures $T_{Mg/Li}$ (Fig. 8). The obtained $T_{Mg/Li}$ values for all MVFs from the Caucasian provinces are in positive correlation with HCO_3^- contents and oxygen isotope compositions (both $\delta^{18}O_{H_2O}$ and $\Delta\delta^{18}O_{H_2O}$) and in high negative correlation with Cl^- (Fig. 8): the Cl^- contents decrease with increasing $T_{Mg/Li}$.

5.2 Constrains of fluid generation depth

The Greater Caucasus backarc basin underwent inversion in the Early Cenozoic induced by the Arabia-Eurasia collision and the Caucasian orogeny. Since that time on, the orogeny has controlled all geological structures and events in the region and its surroundings (Mosar et al., 2010), including the ongoing mud volcanism in south-eastern Europe. It can be illustrated that this control is especially prominent in the eastern part of the region by the case of the Azerbaijan MVs. The Greater Caucasus is a doubly verging fold-thrust belt, with a pro- and a retro wedge actively propagating into the foreland sedimentary basins of Kura in the south and Terek in the north (Fig. 7). The orogenic front of the Greater Caucasus in Azerbaijan lies at the foothills of the Lesser Caucasus, south of the Kura foreland basin (Mosar et al., 2010).

Thus, MVs of the South Caspian province fall within four tectonic units (Fig. 7) with different recent convergence rates and earthquake frequency and magnitudes (Mosar et al., 2010). The Kura basin has the lowest (or locally absent) seismic activity and the thickest crust and Mesozoic-Cenozoic sedimentary fill, whereas the Shemakha-Gobustan and Apsheron areas of Azerbaijan adjacent to the orogenic front are highly seismic and heavily faulted (Aliev, 1985; Guliev et al., 2004). As a consequence, the background conductive heat flux within the South Caspian province is notably higher in the Shemakha-Gobustan and Apsheron areas than in the Kura basin: 50–90 against 20–30 mW/m^2 (Aliev, 1985). The respective geothermal gradient ranges from 13 to 17°C/km (mean value 15°C/km) in the Fore-Kura area and the Baku archipelago to 20–22°C/km (mean value 21°C/km) in the Shemakha-Gobustan and Apsheron areas of Azerbaijan (Aliev, 1985; Guliev et al., 2004).

The large difference in background conductive heat flux leads to differences in fluid generation temperatures ($T_{Mg/Li}$) of MV waters sampled from adjacent areas. The highest values (75°C and 137°C) were inferred for two MVs located in the Fore-Caspian area nearest to the Greater Caucasus Range, which corresponds to a fluid generation depth ($H_{Mg/Li}$) of 3.6 to 6.5 km. Slightly lower average fluid generation temperatures ($T_{Mg/Li}$) were obtained for the Apsheron and Shemakha-Gobustan areas: 63.0±8.6°C and 66.0±7.0°C, respectively (Table 4; Fig. 7), which correspond to an average fluid generation depth of 3.1 km. The $T_{Mg/Li}$ value is much lower (37.5±7.0°C) for MVFs of the Fore-Kura area, the most distant from the Greater Caucasus. However, the average $H_{Mg/Li}$ depth (~2.5 km) is not much shallower than in adjacent Azerbaijan, given the considerably lower regional geothermal gradient. The respective depth intervals in all these areas are occupied by the Maykop shale and younger sediments.

The MV waters sampled in the Taman Peninsula fall into three groups according to the estimated fluid generation

Table 4 Mg/Li temperature and depth constrains for mud volcano reservoirs in the Caucasus region (mean and extreme values, standard deviation)

MV province, area	$T_{Mg/Li}$/°C	$H_{Mg/Li}$/km
Kerch-Taman province	41–137 78.8±11.8 (n = 18)	1.0–3.6 2.0±0.3 (n = 18)
South Caspian province	18–137 60.8±6.3 (n = 59)	0.8–6.5 3.1±0.3 (n = 59)
Fore-Caspian area	75–137 106 (n = 2)	3.6–6.5 5.1 (n = 2)
Apsheron area	48–73 63±8.6 (n = 5)	2.3–3.5 3.0±0.4 (n = 5)
Shemakha-Gobustan area	18–116 66.0±7.0 (n = 39)	0.8–5.5 3.1±0.3 (n = 39)
Fore-Kura area	21–56 37.5±7.0 (n = 13)	1.4–3.7 2.5±0.5 (n = 13)
Kakhety province	58–108 78.3±22.4 (n = 4)	1.9–3.6 2.6±0.8 (n = 4)

Notes: n–number of estimations.

temperatures ($T_{Mg/Li}$) (Fig. 9). The $T_{Mg/Li}$ values are relatively low (41°C to 66°C) in the northern part of the peninsula near the Azov coast, higher (75°C–89°C) in the south, around the Taman Gulf and on the Black Sea coast, and the highest (86°C–137°C) in the extreme east of the peninsula (east of the N–S Djiga fault impacted by the Greater Caucasus orogeny). The temperature zoning is generally oriented in the W–E direction and controlled by the folding pattern in sediments (Shnyukov et al., 1986). Unlike other areas of the Caucasian collisional zone with generally NW-striking folds in Mesozoic-Cenozoic sediments, the folds in the Taman Peninsula are mostly narrow and W–E trending. The MV waters within anticlinal folds in the north of the peninsula, where the Maykop Formation spans the depths from 0.6 to 1.6 km to 2–4 km (Rostovtsev, 2000), originate at $H_{Mg/Li}$ ~1.0–1.5 km, as calculated with reference to a geothermal gradient of ~40°C/km (Lagunova, 1975). The respective fluid generation depths in the southern peninsula part, where the Maykop shale is thicker and lies between ~1.0–2.6 km and 5–7 km (Rostovtsev, 2000), are 1.9–2.2 km. These estimates are consistent with the inference (Shnyukov et al., 1986 and 2005; Kokh et al., 2015; Sokol et al., 2018 and 2019) that MVs in the Kerch and Taman peninsulas feed mainly from the Middle Maykop strata. The group of large MVs east of the Djiga fault is associated with NW folds, especially with the anticlines that have Cretaceous cores (Shnyukov et al., 1986 and 2005). These mud volcanoes have the deepest roots in the peninsula: $H_{Mg/Li}$ ~ 2.2–3.4 km.

6 Conclusions

The Caucasian collision zone, a classical area of intracontinental mud volcanism, comprises two large onshore MV provinces (Kerch-Taman and the Caspian) and a smaller province (Kakhety) between them. The two large units are the Kerch-Taman province in the west and the Caspian one in the east, which are exposed to the influence of the Caucasian orogeny decaying westward and northward. The two provinces differ markedly in total thickness and petroleum potential of sediments correlated with trends in the generation depths of fluids that feed MVs at different sites of the vast territory.

The reported study on the formation conditions of fluids in the Caucasian mud volcanic provinces shows that the MV waters formed within a temperature range of 18°C to 137°C. They are i) hot HCO_3-rich waters with high $\delta^{18}O_{H_2O}$ values and ii) relatively cold chloride waters with lower $\delta^{18}O_{H_2O}$. According to Mg/Li geothermometry, less saline HCO_3/Na-type MV waters generate at greater depths

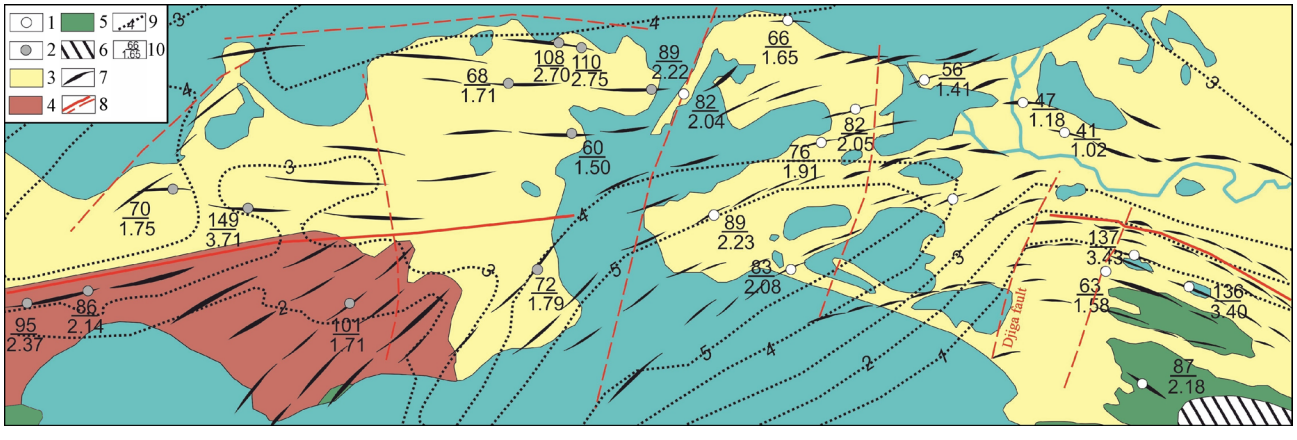

Fig. 9 Constrained MV fluid generation temperatures ($T_{Mg/Li}$) and depths ($H_{Mg/Li}$) of mud volcanic reservoirs of the Kerch-Taman province. Sketch map of the Crimea and Taman Peninsulas modified from Shnyukov et al. (1986). 1-2 – MVs: 1 – authors data, 2 – extra data are according to (Ershov and Levin, 2016; Sokol et al., 2019); 3 – Cenozoic sedimentary strata, 4 – Oligocene-Early Miocene shales (Maykop Formation), 5 – Cretaceous sedimentary strata, 6 – the Greater Caucasus orogeny, 7 – anticlinal folds, 8 – faults; 9 – isopachitis of the Maykop strata, km (Tugolesov, 1985); 10 – ranges of estimated $T_{Mg/Li}$ and $H_{Mg/Li}$ values. The specific values see in Table 2.

than more saline Cl/Na MV waters. The lateral MVF temperature distribution agrees with the patterns of major-ion chemistry and $\delta^{18}O_{H_2O}$ and δD_{H_2O} values. The correlation is especially prominent in the South Caspian MV province. Namely, the HCO_3-Cl/Na-type waters of relatively low salinity formed at higher temperatures than the Cl/Na-type brines. The MVF base temperatures in different Caucasian mud volcanic provinces increase concordantly toward the Great Caucasus Range, this being the evidence of relation between fluid generation conditions and regional tectonic activity (and heat flux). The HCO_3-rich MV waters in the region occur mainly within active tectonic zones, which agrees with the previously revealed global tendency. Taking into account local variations in geothermal gradient, the mud reservoirs can be expected to lie in the depths interval from ~ 0.85 to 6.5 km within Cenozoic sediments, mostly corresponding to the Maykop Formation shales. The temperature and chemistry patterns in MV fluids of the Caucasus region are largely due to sediment maturation at different temperatures and depths.

Acknowledgements We wish to thank Drs. Ad.A. Aliev and A. Guseinov from the Institute of Geology of National Azerbaijan Academy of Sciences (Baku) for assistance in the field investigation, including the sampling of mud volcanoes. The manuscript profited much from the thoughtful review and valuable comments by reviewers, which we have accepted with gratitude. Thanks are extended to B.G. Pokrovskiy from the Institute of Geology of Russian Academy of Sciences (Moscow) for assistance in isotope analysis. The study was supported by grant 17-17-01056 from the Russian Science Foundation.

Electronic Supplementary Material Supplementary material is available in the online version of this article at http://dx.doi.org/10.1007/s11707-019-0810-8 and is accessible for authorized users.

References

Adamia S A (1985). Crust and mantle structure in the Caucasus and its relation to modern geological structures. In: Geophysical Fields and Crust Structure in Transcaucasia. Moscow: Nauka, 151–169 (in Russian)

Adamia S, Mumladze T, Sadradze N, Tsereteli E, Tsereteli N, Varazanashvili O (2008). Late Cenozoic tectonics and geodynamics of Georgia (SW Caucasus). Georgian International Journal of Sciences and Technology, 1: 77–107

Adamia S, Zakariadze G, Chkhotua T, Sadradze N, Tsereteli N, Chabukiani A, Gventsadze A (2011). Geology of the Caucasus: a review. Turk J Earth Sci, 20: 489–544

Aliev Ad A, Bairamov A A (2007). Space and time patterns of mud volcanism in Azerbaijan in the context of a new tectonic model. Transactions, IG NAN Azerbaijan, 35: 25–45 (in Russian).

Aliyev A A, Guliyev I S, Rakhmanov R R (2009). Catalogue of Mud Volcanoes Eruptions of Azerbaijan: 1810–2007. Baku: Nafta Press, 1–109

Aliyev A A, Guliyev I S, Dadashev F G, Rakhmanov R R (2015) Atlas of the World Mud Volcanoes. Baku: Nafta Press

Aliev S (1985). Map of Heat Flows in Basins of Azerbaijan, Scaled 1:500000. Moscow: Mingeo SSSR (in Russian)

Ali-Zade Ak A (2008). Geology of Azerbaijan. Book VII. Oil and Gas. Baku: Nafta Press, 1–672 (in Russian)

Bödvarsson G (1961). Physical characteristics of natural heat resources in Iceland. In: UN Conference on new sources of energy. Rome: 1–19

Bödvarsson G, Pálmason G (1961). Exploration of subsurface temperatures in Iceland. Jokull, 11: 39–48

Chelidze T L (1983) Thermodynamic environments and petrophysical models of regions of the earth's crust in the Caucasus. In: Chikovani D S, Lursmanashvili O V, eds. The structure of the Georgia earth crust inferred from seismic and magnetic data. (Proceed. Geophysics Institute of the Georgian Acad. of Sci., 51). Tbilisi: Metsniereba, 97–115 (in Russian)

Chelnokov G A, Bragin I V, Kharitonova N A (2018). Geochemistry of mineral waters and associated gases of the Sakhalin Island (Far East of Russia). J Hydrol (Amst), 559: 942–953

Craig H (1961). Isotopic variation in meteoric waters. Science, 233: 133–149

Craig H (1963). The isotope geochemistry of water and carbon in geothermal areas. In: Tongiorgi E, ed. Nuclear Geology on Geothermal Areas. Pisa: Spoleto, 17–53

Dählmann A, de Lange G J (2003). Fluid-sediment interactions at Eastern Mediterranean mud volcanoes: a stable isotope study from ODP Leg 160. Earth Planet Sci Lett, 212(3–4): 377–391

D'Amore F, Arnórsson S (2000). Geothermometry. In: Arnórsson S, ed. Isotopic and Chemical Techniques in Geothermal Exploration, Development and Use. Sampling Methods, Data Handling, Interpretation. Vienna: International Atomic Energy Agency, 152–199

Dimitrov L (2002). Mud volcanoes as the most important pathways for degassing deeply buried sediments. Earth Sci Rev, 59(1–4): 49–76

Dubinin A V, Dubinina E O (2014). Isotope composition of oxygen and hydrogen in the Black Sea waters as a result of the dynamics of water masses. Oceanology (Mosc), 54(6): 713–729

Dubinina E O, Kovalenker V A, Avdeenko A S, Lavrushin V Yu, Stepanets M I (2005). Origin of mineral springs of the Elbrus region, northern Caucasus: isotopic-geochemical evidence. Geochem Int, 43 (10): 988–998

Dubinina E O (2013). Stable isotopes of light elements in rock-fluid interactions and contamination. Dissertation for the Doctoral Degree. Moscow: IGEM, 1–50 (in Russian)

Ershov V V, Levin B V (2016). New data on the material composition of mud volcano products on Kerch Peninsula. Dokl Earth Sci, 471(1): 1149–1153

Ershov V V, Nikitenko O A, Perstneva Yu A (2016). Geochemistry of mud and fluid migration in mud volcanoes. Vestnik of the Far East Branch of the Russian Academy of Sciences, 5(189): 52–58 (in Russian)

Etiope G (2015). Natural Gas Seepage. The Earth's Hydrocarbon Degassing. Switzerland: Springer

Ferronsky V I, Polyakov V A (2012). Isotopes of the Earth's Hydrosphere. Berlin: Springer

Feyzullayev A A (2012). Mud volcanoes in the South Caspian basin: nature and estimated depth of its products. Nat Sci, 4(07): 445–453

Fouillac C, Michard G (1981). Sodium/litium ratio in water applied to geothermometry of geothermal reservoirs. Geothermics, 10(1): 55–

70

Fournier R O (1977). Chemical geothermometers and mixing models for geothermal systems. Geothermics, 5(1–4): 41–50

Fournier R O, Truesdell A H (1973). An empirical Na K Ca chemical geothermometer for natural waters. Geochim Cosmochim Acta, 37 (5): 1255–1275

Gamkrelidze I P, Giorgobiani T V (1989). Problems of Alpian deformation in the Greater Caucasus and adjacent areas. In: Milanovskii E E, Koronovskii N V, eds. Geology and Mineral Resources of the Greater Caucasus. Moscow: Nauka, 35–40 (in Russian)

Gieskes J M, You C F, Lee T, Yui T F, Chen H W (1992). Hydrogeochemistry of mud volcanoes in Taiwan. Acta Geologica Taiwanica, 30: 79–88

Giggenbach W F (1995). Variations in the chemical and isotopic composition of fluids discharged from the taupo volcanic zone, New Zealand. J Volcanol Geotherm Res, 68(1–3): 89–116

Guliev I S, Dadashev F G, Poletaev A V (2013). Isotopes of Hydrocarbon Gases in Azerbaijan. Baku: Nafta Press (in Russian)

Guliev I S, Huseynov D A, Feizullaev A A (2004). Fluids of mud volcanoes in the Southern Caspian sedimentary basin: geochemistry and sources in light of new data on the carbon, hydrogen, and oxygen isotopic compositions. Geochem Int, 42(7): 688–695

Guliev I S, Kadirov F A, Reilindzher R E (2002). Active tectonics of Azerbaijan: dased on geodesical, gravimetric, and seismic data. Dokl Earth Sci, 382(6): 812–815

Guliev I S, Pavlenko N I, Radjabov M M (1988). Zones of regional decompaction in the South Caspian basin sedimentary cover. Lithol Miner Resour, 5: 130–136

Horn R A (1969). Marine Chemistry. The Structure of Water and the Chemistry of the Hydrosphere. New York: Willey-Interscience

Iosseliani M S, Diasamidze S P (1983). Compiling seismic model of the earth crust in Georgia intermountain depression. In: Chikovani D S, Lursmanashvili O V, eds. The Structure of the Georgia Earth Crust Inferred from Seismic and Magnetic Data. (Proceed. Geophysics Institute of the Georgian Acad. of Sci., 51). Tbilisi: Metsniereba, 34–42 (in Russian)

Jakubov A A, Alizade A A, Zeinalov M M (1971). Mud volcanoes of Azerbaijan. Baku: Publ. AN Azerbaijan, 1–258 (in Russian)

Jakubov A A, Grigoryants B V, Aliev A D, Babazade A D, Veliev M M, Gadzhiev Ya A, Guseinzade I G, Kabulova A Ya, Kastryulin N S, Matanov F A, Mustafaev M G, Rakhmanov R R, Safarova O B, Seidov A G (1980). Mud Volcanism in the USSR Territory and Its Relation with Petroleum Potential. Baku: Elm, 1–167 (in Russian)

Kadirov F A, Floyd M, Reilinger R, Alizadeh Ak A, Guliyev I S, Mammadov S G, Safarov R T (2015). Active geodynamics of the Caucasus region: implications for earthquake hazards in Azerbaijan. Proceed. of Azerbaijan National Academy of Sciences. Sciences of Earth, 3: 3–17

Karandashev V K, Leikin A Y, Khvostikov V A, Kutseva N K, Pirogova S V (2016). Water analysis by inductively coupled plasma mass spectrometry. Inorg Mater, 52(14): 1391–1404

Kharaka Y K, Mariner R H (1989). Chemical geothermomethers and their application to formation waters from sedimentary basins. In: Naeser N D, McCulloch T H, eds. Thermal History of Sedimentary Basins, Methods and Case Histories. New York: Springer-Verlag, 99–117

Khain V E (1982). Tectonic history of the Greater Caucasus in fixistic and mobilistic models. Geotectonics, 4: 3–13 (in Russian)

Kholodov V N (2002). Mud volcanoes: distribution and genesis: communication 1. Mud-volcanic provinces and morphology of mud volcanoes. Lithol Miner Resour, 37(3): 197–209

Kholodov V N (2013). Distribution and formation conditions of salt diapirs and mud volcanoes. Lithol Miner Resour, 48(5): 398–415

Kikvadze O E, Lavrushin V Y, Pokrovskii B G, Polyak B G (2014). Isotope and chemical composition of gases from mud volcanoes in the Taman Peninsula and problem of their genesis. Lithol Miner Resour, 49(6): 491–504

Kokh S N, Shnyukov Y F, Sokol E V, Novikova S A, Kozmenko O A, Semenova D V, Rybak E N (2015). Heavy carbon travertine related to methane generation: a case study of the Big Tarkhan cold spring, Kerch Peninsula, Crimea. Sediment Geol, 325: 26–40

Kokh S N, Sokol E V, Dekterev A A, Kokh K A, Rashidov T M, Tomilenko A A, Bul'bak T A, Khasaeva A, Guseinov A (2017). The 2011 strong fire eruption of Shikhzarli mud volcano, Azerbaijan: a case study with implications for methane flux estimation. Environ Earth Sci, 76(20): 701

Kopf A, Deyhle A, Lavrushin V Yu, Polyak B G, Gieskes J M, Buachidze G I, Wallmann K, Eisenhauer A (2003). Isotopic evidence (He, B, C) for deep fluid and mud mobilization from mud volcanoes in the Caucasus continental collision zone. International Journal of Earth Sciences. Geol Rundsch, 92: 407–425

Kopf A J (2002). Significance of mud volcanism. Rev Geophys, 40(2): 1005–1012

Krasnopevtseva G V, Rezanov I A, Shevchenko V I (1977). Deep structure, seismic interfaces, and crust evolution in the Caucasus. In: Crust and Mantle Structure, from Seismic Data. Kiev: Naukova Dumka, 203–216 (in Russian)

Lagunova, I A (1975). Genesis of Boron in waters of mud volcanoes. Sov, 1975, 1: 147–152 (in Russian)

Lagunova I A, Gemp S D (1971). Chemistry of mud volcanic waters in the Kerch-Taman province. In: Hydrogeology and Geological Role of Groundwaters. Leningrad: Leningrad University, 201–210 (in Russian)

Lagunova I A, Gemp S D (1978). Water chemistry of mud volcanoes. Sovetskaya Geologiya, 8: 108–125 (in Russian)

Lavrushin V Yu, Polyak B G, Prasolov R M, Kamenskii I L (1996). Sources of material in mud volcano products (based on isotopic, hydrochemical, and geological data). Lithol Miner Resour, 31(6): 557–578

Lavrushin V Yu (2012). Subsurface fluids of the Greater Caucasus and its surroundings (Transactions, GIN, Issue 599). Moscow: GEOS (in Russian)

Lavrushin V Yu, Kopf A, Deyhle A, Stepanets M I (2003). Formation of mud-volcanic fluids in Taman (Russia) and Kakhetia (Georgia): evidence from boron isotopes. Lithol Miner Resour, 38(2): 120–153

Lavrushin V Yu, Dubinina E O, Avdeenko A S (2005). Isotopic composition of oxigen and hydrogen in mud-volcanic waters from Taman (Russia) and Kakhetia (Eastern Georgia). Lithol Miner Resour, 40(2): 123–137

Lavrushin V Y, Guliev I S, Kikvadze O E, Aliev A A, Pokrovsky B G, Polyak B G (2015). Waters from mud volcanoes of Azerbaijan:

isotopic-geochemical properties and generation environments. Lithol Miner Resour, 50(1): 1–25

Leonov Yu G (2007). The Greater Caucasus in the Alpine Epoch. Moscow: GEOS (in Russian)

Mazzini A, Svensen H, Planke S, Guliyev I, Akhmanov G G, Fallik T, Banks D (2009). When mud volcanoes sleep: insight from seep geochemistry at the Dashgil mud volcano, Azerbaijan. Mar Pet Geol, 26(9): 1704–1715

Mazzini A, Etiope G (2017). Mud volcanism: an updated review. Earth Sci Rev, 168: 81–112

Milanovskii E E, Koronovskii N V (1973). Orogenic Volcanism and Tectonics of the Alpine Belt of Eurasia. Moscow: Nedra, 1–279 (in Russian)

Milkov A V (2000). Worldwide distribution of submarine mud volcanoes and associated gas hydrates. Mar Geol, 167(1–2): 29–42

Mosar J, Kangarli T, Bochud M, Glasmacher U A, Rast A, Brunet M F, Sosson M (2010). Cenozoic-Recent tectonics and uplift in the Greater Caucasus: a perspective from Azerbaijan. Geol Soc Lond Spec Publ, 340(1): 261–280

Nadirov R S, Bagirov E, Tagiyev M, Lerche I (1997). Flexural plate subsidence, sedimentation rates, and structural development of the super-deep South Caspian Basin. Mar Pet Geol, 14(4): 383–400

Olenchenko V V, Shnyukov Y F, Gas'kova O L, Kokh S N, Sokol E V, Bortnikova S B, El'tsov I N (2015). Explosion dynamics of the Andrusov mud vent (Bulganak mud volcano area, Kerch Peninsula, Russia). Dokl Earth Sci, 464(1): 951–955

Oppo D, Capozzi R, Nigarov A, Esenov P (2014). Mud volcanism and fluid geochemistry in the Cheleken peninsula, western Turkmenistan. Mar Pet Geol, 57: 122–134

Philip H, Cisternas A, Gvishiani A, Gorshkov A (1989). The Caucasus: an actual example of the initial stages of continental collision. Tectonophysics, 161(1-2): 1–21

Pokrovsky B G, Zaviyalov P O, Bujakaite M I, Izhitskiy A S, Petrov O L, Kurbaniyazov A K, Shimanovich V M (2017). Geochemistry of O, H, C, S, and Sr isotopes in the water and sediments of the Aral Basin. Geochem Int, 55(11): 1033–1045

Radzhabov M M, Osipova I B, Armenakyan K H, Ioseliani M S, Diasamidze S P, Shcherbakov V V, Kutsenko E Ya, Votsalevsky Z S (1985). Wave fields and deep structure of the Caucasus according to seismic data. In: Geophysical Field and Crustal Structure of the Caucasus. Moscow: Nauka, 5–33 (in Russian)

Rakhmanov R R (1987). Mud Volcanoes: Implications for Petroleum Reservoir Potential. Moscow: Nedra (in Russian)

Revil A (2002). Genesis of mud volcanoes in sedimentary basins: a solitary wave-based mechanism. Geophys Res Lett, 29(12): 1574

Reilinger R, McClusky S, Vernant P, Lawrence S, Ergintav S, Cakmak R, Ozener H, Kadirov F, Guliev I, Stepanyan R, Nadariya M, Hahubia G, Mahmoud S, Sakr K, ArRajehi A, Paradissis D, Al-Aydrus A, Prilepin M, Guseva T, Evren E, Dmitrotsa A, Filikov S V, Gomez F, Al-Ghazzi R, Karam G (2006). GPS constraints on continental deformation in the Africa-Arabia-Eurasia continental collision zone and implications for the dynamics of plate interactions. J Geophys Res Solid Earth, 111: 1–26

Rostovtsev K O (2000). The Geological Map of the Russian Federation, Scaled 1:200 000. Caucasian Series, Sheets L-37-XIX, L-37-XXV (Taman). FGUGP "Caucasus geological survey", NGO "Yuzhmorgeologiya" Publisher: VSEGEI

Seletskii Yu B (1991). Deuterium and oxygen-18 in the context of mud volcanic waters formation. Izvestia AN SSSR. Geology, 5: 133–138 (in Russian)

Seletskii Yu B (1998). Condensation and solution waters of oil and gas fields: possible mechanisms of formation of their isotopic composition. Water Resour, 25(3): 259–264

Shnyukov E F, Sobolevskiy Yu V, Gnatenko G I, Naumenko P I, Kutniy V A (1986). Mud volcanoes of the Kerch-Taman region: an atlas. Kiev: Naukova Dumka, 1–152 (in Russian).

Shnyukov E, Sheremetiev V, Maslakov N, Kutniy V, Gusakov I, Trofimov V (2005). Mud Volcanoes of the Kerch-Taman Region. Krasnodar: Glav Media Publishing House (in Russian)

Sobissevitch A L, Gorbatikov A V, Ovsuchenko A N (2008). Deep structure of the Mt. Karabetov mud volcano. Dokl Earth Sci, 422(1): 1181–1185

Sokol E, Kokh S, Kozmenko O, Novikova S, Khvorov P, Nigmatulina E, Belogub E, Kirillov M (2018). Mineralogy and geochemistry of mud volcanic ejecta: a new look at old issues (A case study from the Bulganak field, Northern Black Sea). Minerals (Basel), 8(8): 344

Sokol E V, Kokh S N, Kozmenko O A, Lavrushin V Yu, Belogub E V, Khvorov P V, Kikvadze O E (2019). Boron in an onshore mud volcanic environment: case study from the Kerch Peninsula, the Caucasus continental collision zone. Chem Geol, 525: 58–81

Tugolesov D A, Gorshkov A S, Meisner L B, Solov'ev V V, Khakhalev E M (1985). Tectonics of Mesozoic–Cenozoic Deposits of the Black Sea Basin. Moscow: Nedra, 1–215 (in Russian)

Vetshtei`n V E (1982). Oxygen and Hydrogen Isotopes in Natural Waters of the USSR. Leningrad: Nedra, 1–216 (in Russian)

You C F, Gieskes J M, Lee T, Yui T F, Chen H W (2004). Geochemistry of mud volcano fluids in the Taiwan accretionary prism. Appl Geochem, 19(5): 695–707

Zonenshain L P, Pichon X (1986). Deep basins of the Black Sea and Caspian Sea as remnants of Mesozoic back-arc basins. Tectonophysics, 123(1–4): 181–211

AUTHOR BIOGRAPHIES

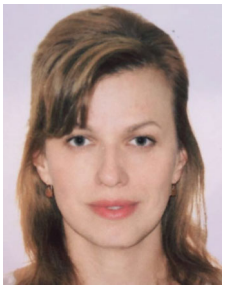

Dr. Olga Evgenievna Kikvadze is working in the Geological Institute of the Russian Academy of Sciences, Moscow, Russia, in the position of Senior Scientific Worker. In 2016, she defended the Ph.D Thesis for (Candidate of Geology and Mineralogy Sciences) on the topic "Geochemistry of mud volcano fluids in Caucasus region."

She published personally and in cooperation with colleagues 22 papers in Russian and foreign editions. Her current and previous research interests: hydrogeology, geochemistry and isotope geochemistry.

Both of co-authors have the degree of Ph.D of Science (Geology and Mineralogy) and are working in the same Geological Institute of Russian Academy of Sciences, Moscow, Russia.

E-mail: bolik2000@mail.ru